# The generalized log-derivative method for evaluation of second-order transition amplitudes

Felicja Mrugała
*Institute of Physics, Nicholas Copernicus University, Grudziadzka 5/7, 87-100 Torun, Poland*

(Received 21 October 1988; accepted 6 March 1989)

The log-derivative method of Johnson is generalized to calculate matrix elements of multichannel Green's functions—second-order transition amplitudes—which arise from description of a variety of physical processes involving weak interactions of initial and final (bound) states with a set of strongly coupled continuum and/or bound intermediate states. A purely approximate-solution algorithm and two hybrid approximate-solution approximate-potential versions, based on the use of piecewise constant reference potentials, are presented and tested on problems concerning investigations of nonadiabatic effects in the spectroscopy of $H_2$. A comparison with the renormalized Numerov method, extended to calculation of considered transition amplitudes, is made and superior efficiency of the hybrid log-derivative algorithms is demonstrated. It is shown both practically and theoretically that discretization errors of the hybrid algorithms grow linearly with increasing energy in calculations, whereas cubic growth of errors with energy is characteristic for the purely approximate-solution log-derivative and Numerov algorithms.

## I. INTRODUCTION

As pointed out in the recent paper by Singer *et al.*,[1] there are many physical processes amenable to treatment in second-order perturbation theory which involve (weakly allowed) transitions through a manifold of strongly coupled continuum or/and bound states and are quantitatively described by matrix elements between initial and final state functions of a multichannel Green's function connected with the Schrödinger equation for the intermediate states. Hence, developing stable and efficient algorithms for numerical evaluation of these matrix elements—second-order transition amplitudes—is a task of general importance.

Intending to employ a step-by-step integrator to a multichannel Schrödinger equation one has to remember, of course, on some precautions against the loss of linear independence of solutions in classically forbidden regions. Since not only regular but also irregular solutions are involved in evaluation of the second-order transition amplitudes, the necessity of maintaining the linear independence between these solutions arises in addition to the usual stability requirements of standard scattering calculations ($S$-matrix evaluations). Stressing this fact Singer *et al.*[1] propose to meet the additional requirement by modifying the boundary conditions for irregular solutions at each integration step in a way dependent on behavior of stabilized regular solutions, generated simultaneously. This proposal is a generalization of the standard stabilization techniques which were applied before only to solutions of one (usually regular) kind. Following it, the authors develop a general stable scheme for evaluation of second-order transition amplitudes and show how within this scheme the established scattering methods, like the $R$-matrix propagation[2] and the renormalized Numerov[3] methods, can be exploited.

In the present paper, another approach to numerical evaluation of second-order transition amplitudes is proposed. The amplitudes are viewed as integrals of products of two functions, one of which represents the final state and its coupling to the intermediate states and the second function describes motion on the intermediate states driven by transitions from the initial state. Functions of the latter type are determined as solutions of appropriate two-point boundary value problems for inhomogeneous coupled differential equations. Numerical instabilities, being the matter of main concern in Ref. 1, are completely circumvented in treatment of these problems by making a consequent use of the invariant imbedding concept.[4,5] More attention is given instead to efficiency in evaluation of the quantities of interest.

Algorithms are derived on the basis of the inherently stable $L$-matrix formulation of two-potential scattering problems introduced previously[6] in connection with evaluation of first-order transition amplitudes. In Sec. II, this formalism is supplied with a recurrence relation necessary for propagation of second-order amplitudes. Simultaneously with these amplitudes, two related first order amplitudes and a log-derivative matrix have to be propagated. The complete set of the recurrence relations involves, beside the basic $L$-matrix propagator, quantities which are essentially counterparts of the first- and second-order amplitudes defined for small sectors of the entire propagation range. Formulas for evaluation of these sector quantities have to be provided, of course, in order to fully specify the way of evaluation of the global quantities. Accuracy and efficiency of the final algorithm critically depend on the approach chosen at this stage of its derivation.

The approximate-solution type discretization procedure of integral equations which was used in the derivation of the original and of the generalized log-derivative methods[6–9] to obtain approximate expressions for the sector and, subsequently, for the half-sector $L$ matrices and first-order amplitudes is employed and extended in Sec. III to give the needed expressions for second-order amplitudes. Modification of this procedure, consisting in the use of piecewise constant diagonal reference potentials and thereby admixing

 0021-9606/89/140874-16$02.10 

some approximate-potential features to it, has been demonstrated recently[10,11] to improve efficiency of the original algorithm of Johnson. The same modification and its extension to driven equations (consisting in the use of piecewise constant reference inhomogeneities) are considered also in Sec. III for enhancing efficiency of the approximate-solution approach in evaluation of first- and second-order amplitudes. As a result, three new log-derivative related algorithms are developed for evaluation of second-order amplitudes: one of purely approximate-solution type and two having hybrid approximate-solution approximate-potential character.

The new algorithms have been already exploited and found useful in the calculations concerning the realistic problem of predissociation of the $D\ ^1\Pi_u^+$ state of $H_2$ by photon impact, reported in Ref. 12. No computational details were enclosed, however, in this report. An extensive description of performance of the new algorithms in exemplary application to investigation of some nonadiabatic effects in the spectroscopy of $H_2$ is given in Sec. IV. A model of the $H_2$ molecule is constructed on which, at first (Sec. IV A), the way of implementation of the log-derivative algorithms to predissociation calculations, being carried out in both perturbative and nonperturbative approaches, is demonstrated. Then, accuracy of the nonhybrid and of the hybrid versions of these algorithms is compared in calculations of two predissociation profiles which appear in the cross section for the photodissociation of $H_2$ (model) molecule from the ground state into the $H(n=1)+H(n=2)$ channel at energies just above and well above the threshold, respectively. In Sec. IV B, the energy range below this dissociation limit is taken into consideration and the methodology of investigation of predissociating (i.e., resonance) states, followed in Sec. IV A, is adapted to bound state calculations. In particular, a nonperturbative procedure of determination of nonadiabatic energy shifts of bound rovibrational states is suggested in which advantages are taken of numerical stability of the new methods in one-way propagation of second-order transition amplitudes. The amplitudes evaluated in the course of searching for a nonadiabatic energy level involve the eigenfunction of the corresponding adiabatic level. The procedure is initially tested (in Sec. IV B) on the model molecule for consistency of results with perturbation theory predictions in cases involving small nonadiabatic interactions. Its adequacy in treatment of the real molecule is finally documented in Sec. V where results obtained for nonadiabatic shifts of selected rovibrational levels in the $B\ ^1\Sigma_u^+$, $B'\ ^1\Sigma_u^+$, $C\ ^1\Pi_u$, and $D\ ^1\Pi_u$ states of $H_2$ are shown to agree satisfactorily with the values calculated for these shifts in Ref. 13, using the renormalized Numerov method.[3] In the remainder of Sec. IV B, numerical tests on the model molecule are described which illustrate differences in performance between the nonhybrid and the hybrid algorithms in the bound state calculations. A comparison is also made of the new log-derivative algorithms with a Numerov-related scheme of evaluation of second-order amplitudes, presented in Appendix A.

All the algorithms considered are of the same, fourth, order. The important difference between them concerns behavior of errors with increasing energy in calculations. It is observed in the tests that errors of results generated by the hybrid log-derivative algorithms grow linearly with energy, whereas errors of results obtained by the purely approximate-solution log-derivative and the Numerov algorithms reveal a rapid cubic growth with energy. These observations are confirmed theoretically in an analysis of local discretization errors in the hybrid and in the nonhybrid versions of the log-derivative algorithm, given in Appendix B. Accuracy tests of the algorithms, completed with a count of matrix operations required at a single integration step, are concluded with an estimate of their relative efficiency: the nonhybrid version of the log-derivative algorithm is estimated to be comparable with the Numerov algorithm in evaluation of second-order transition amplitudes regardless of the value of energy involved and the hybrid versions are found to be superior to both the purely approximate-solution type algorithms in high energy calculations.

No direct comparison is made with the methods proposed in Ref. 1 since superior efficiency of the new log-derivative related algorithms seems to be guaranteed by simplicity of their formulas.

## II. SECOND-ORDER TRANSITION AMPLITUDES IN THE *L*-MATRIX FORMULATION

Let us consider a real Hermitian $N\times N$ matrix operator $D$;

$$D:=Id^2/dx^2+B(x) \tag{1}$$

and the following three boundary value problems for it:

$$D\psi^{\alpha}_{x',x''}(x)=\delta_{\alpha,0}\phi(x) \quad \text{for } \alpha=+,-,0, \tag{2}$$

$$\psi^{\pm}_{x',x''}(x')=\begin{cases} I \\ 0 \end{cases}, \quad \psi^{\pm}_{x',x''}(x'')=\begin{cases} 0 \\ I \end{cases},$$

$$\psi^{0}_{x',x''}(x')=\psi^{0}_{x',x''}(x'')=0, \tag{2a}$$

with $\phi(x)$ being an $N\times N_0$ matrix of given functions and with $I$ denoting the $N\times N$ unit matrix.

Let us define the following integrals;

$$J^{\alpha}_{x',x''}:=\langle\psi^{\alpha}_{x',x''},\phi\rangle \quad \text{for } \alpha=+,-,0, \tag{3}$$

where

$$\langle Y_{a,b},Z\rangle:=\int_a^b Y^T_{a,b}(x)Z(x)dx,$$

involving solutions of these problems, $\underset{N\times N}{\psi^{\pm}_{x',x''}}$ and $\underset{N\times N_0}{\psi^{0}_{x',x''}}$. In terms of the same functions are also defined the $2N\times 2N$ matrix $L_{x',x''}$,

$$L_{x',x''}:=\begin{pmatrix} L^{(1)}_{x',x''} & L^{(2)}_{x',x''} \\ L^{(3)}_{x',x''} & L^{(4)}_{x',x''} \end{pmatrix};$$

$$L_{x',x''}:=\begin{pmatrix} \dot\psi^{+}_{x',x''}(x') & \dot\psi^{-}_{x',x''}(x') \\ \dot\psi^{+}_{x',x''}(x'') & \dot\psi^{-}_{x',x''}(x'') \end{pmatrix}, \tag{4}$$

and the $N\times N_0$ matrices $T_{x',x''}$ and $Q_{x',x''}$;

$$T_{x',x''}:=\dot\psi^{0}_{x',x''}(x''), \quad Q_{x',x''}:=\dot\psi^{0}_{x',x''}(x'), \tag{5}$$

introduced and exploited in Refs. 8 and 6 as a set of invariant imbedding type quantities propagating any solution of equation

$$D\psi=\phi$$

across an interval $[x',x'']$. ($x''\geqslant x'$ is assumed for definiteness.) The respective propagation relation reads

$$\begin{pmatrix}\dot{\psi}(x')\\ \dot{\psi}(x'')\end{pmatrix}=L_{x',x''}\begin{pmatrix}\psi(x')\\ \psi(x'')\end{pmatrix}+\begin{pmatrix}Q_{x',x''}\\ T_{x',x''}\end{pmatrix}. \tag{6}$$

(Overdot denotes derivative with respect to $x$.) The $J^{\pm}_{x',x''}$ integrals introduced here are simply related to the matrices $T_{x',x''}$ and $Q_{x',x''}$:

$$J^{+}_{x',x''}=-Q_{x',x''},\quad J^{-}_{x',x''}=T_{x',x''}\ , \tag{7}$$

which becomes apparent if one (i) rewrites the problem (2) and (2a) for the function $\psi^0_{x',x''}$ in the integral form

$$\psi^0_{x',x''}=G^0_{x',x''}\phi\ ,$$

i.e.,

$$\psi^0_{x',x''}(x)=\int_{x'}^{x''}G^0_{x',x''}(x,y)\phi(y)dy\ ,$$

using the appropriate Green's function $G^0_{x',x''}(x,y)$;

$$D(x)G^0_{x',x''}(x,y)=I\delta(x-y)\ , \tag{8}$$

$$G^0_{x',x''}(x',y)=G^0_{x',x''}(x'',y)=0\ , \tag{8a}$$

(ii) expresses this Green's function in terms of the solutions $\psi^{+}_{x',x''}$ and $\psi^{-}_{x',x''}$;

$$G^0_{x',x''}(x,y)=\begin{cases}\psi^{-}_{x',x''}(x)(W^{-1}_{x',x''})^T[\psi^{+}_{x',x''}(y)]^T & \text{for } x<y\\ \psi^{+}_{x',x''}(x)W^{-1}_{x',x''}[\psi^{-}_{x',x''}(y)]^T & \text{for } x>y\end{cases}, \tag{9}$$

and (iii) exploits for the Wronskian of these solutions;

$$W_{x',x''}:=W[\psi^{-}_{x',x''},\psi^{+}_{x',x''}],\quad W[\varphi,\chi]:=\varphi^T\dot{\chi}-\dot{\varphi}^T\chi\ , \tag{9a}$$

the following equalities, resulting from the assumed properties of the operator $D$;

$$W[\psi^{-}_{x',x''},\psi^{+}_{x',x''}]=-(L^{(2)}_{x',x''})^T=L^{(3)}_{x',x''}\ . \tag{9b}$$

From hermiticity and reality of $D$ follows also symmetry of the log-derivative matrix $L^{(4)}_{x',x''}$ and of the matrix $L^{(1)}_{x',x''}$ (cf. Ref. 9).

The integral $J^0_{x',x''}$, expressed through the function $G^0_{x',x''}$, takes the form of a "second-order transition amplitude" (more precisely, of an $N_0\times N_0$ matrix of such amplitudes);

$$J^0_{x',x''}=\langle\phi,G^0_{x',x''}\phi\rangle\ . \tag{10}$$

A more general integral of this form

$$J_{x',x''}:=\langle\phi,G_{x',x''}\phi\rangle\ ,$$

with the Green's function satisfying inhomogeneous boundary conditions instead of the conditions (8a);

$$G_{x',x''}(x',y)=0,\quad G_{x',x''}(x,y)=O(x)g^T(y)\quad \text{for } x\geqslant x''\ , \tag{8b}$$

where $O$ denotes an $N\times N$ matrix solution of the equation: $DO(x)=0$ in the range of $x$ outside the $x''$ boundary of $[x',x'']$, can be obtained from the integral $J^0_{x',x''}$ by exploiting the relation

$$J_{x',x''}=T^T_{x',x''}[L_0-L^{(4)}_{x',x''}]^{-1}T_{x',x''}+J^0_{x',x''}\ , \tag{11}$$

where

$$L_0:=\dot{O}(x'')[O(x'')]^{-1}\ . \tag{11a}$$

This relation can be easily proved by making use of the following expressions for the function $\psi_{x',x''}$, $\psi_{x',x''}:=G_{x',x''}\phi$, and its derivative

$$\psi_{x',x''}(x)=\psi^{-}_{x',x''}(x)O(x'')C+\psi^0_{x',x''}(x)\ ,$$

$$\dot{\psi}_{x',x''}(x'')=\dot{O}(x'')C=L^{(4)}_{x',x''}O(x'')C+T_{x',x''}\ ,$$

where

$$C:=\langle g,\phi\rangle\ .$$

Of crucial importance for the derivation of algorithms presented in the next section are the following recurrence relations for "addition" of the $L^{(4)}$, $T$, and $J^0$ matrices defined in the subintervals $[x',y]$ and $[y,x'']$ of the interval $[x',x'']$;

$$L^{(4)}_{x',x''}=L^{(4)}_{y,x''}-L^{(3)}_{y,x''}l(x',y,x'')L^{(2)}_{y,x''}\ , \tag{12a}$$

$$T_{x',x''}=T_{y,x''}-L^{(3)}_{y,x''}l(x',y,x'')[T_{x',y}-Q_{y,x''}]\ , \tag{12b}$$

$$J^0_{x',x''}=J^0_{x',y}+J^0_{y,x''}-[T_{x',y}-Q_{y,x''}]^T\times l(x',y,x'')[T_{x',y}-Q_{y,x''}]\ , \tag{12c}$$

where

$$l(x',y,x''):=[L^{(4)}_{x',y}-L^{(1)}_{y,x''}]^{-1}\ . \tag{12d}$$

The first relation was given in Ref. 8, the second in Ref. 6, and the third relation is new. It is derived by inserting into the defining equation (3) with $\alpha=0$ the following expressions for the function $\psi^0_{x',x''}$:

$$\psi^0_{x',x''}(x)=\psi^0_{x',y}(x)+\psi^{-}_{x',y}(x)a^{-}_{x',y}\quad \text{for } x\in[x',y]\ ,$$

$$\psi^0_{x',x''}(x)=\psi^0_{y,x''}(x)+\psi^{+}_{y,x''}(x)a^{+}_{y,x''}\quad \text{for } x\in[y,x'']$$

with

$$a^{-}_{x',y}=a^{+}_{y,x''}=-l(x',y,x'')[T_{x',y}-Q_{y,x''}]\ ,$$

which relate the solution $\psi^0_{x',x''}(x)$ in the interval $[x',x'']$ to the basic solutions $\psi^{\alpha}_{[p]}(x)$, $\alpha=+,-,0$, in the subintervals $[p]=[x',y]$ and $[p]=[y,x'']$. The coefficients occurring in these expressions result from the continuity of the function $\psi^0_{x',x''}$ and its derivative $\dot{\psi}^0_{x',x''}$ at the common boundary of both subintervals, from the form of the boundary conditions satisfied by the respective solutions $\psi^{\alpha}_{[p]}(x)$ [cf. Eq. (2a)], from the definitions (4) and (5), and from the relations (12a), (12b), and (12d).

In the limit of $(y-x'')\to 0$ the recurrence relations take the form of the following differential equations:

$$\frac{d}{dy}L^{(4)}_{x',y}=-B(y)-(L^{(4)}_{x',y})^2\ , \tag{13a}$$

$$\frac{d}{dy}T_{x',y}=\phi(y)-L^{(4)}_{x',y}T_{x',y}\ , \tag{13b}$$

$$\frac{d}{dy}J^0_{x',y}=-T^T_{x',y}T_{x',y}\ . \tag{13c}$$

These equations together with the initial conditions

$$(L^{(4)}_{x',x'})^{-1}=0,\quad T_{x',x'}=0,\quad J^0_{x',x'}=0 \tag{13d}$$

might be used, in principle, for determining the matrix $J^0_{x',x''}$ (and the matrices $T_{x',x''}$ and $L^{(4)}_{x',x''}$, at the same time). However, direct integration of the differential equations (13a)–(13c) is very impractical, if not impossible (without including additional equations, at least) because of the singulari-

ties of the log-derivative matrix $L^{(4)}_{x',y}$ (and of all other quantities related to it) occurring at some isolated points $y_{\text{sing}}$ of the integration range in most cases of interest.[14] The use of the recurrence relations (12a)–(12d) instead allows bypassing these singularities without affecting the accuracy of the quantities obtained at the end of the interval $[x',x'']$, provided the endpoint $x''$ lies not too close to any $y_{\text{sing}}$ point. This stability is, in fact, an inherent property of the invariant imbedding approach, irrespective of whether it is applied to continuous (as here) or to discrete boundary value problems, and irrespective of specific choice of the propagator (the $L$ matrix, the $R$ matrix, or others[15]). An analytical proof of this property is given, e.g., in Ref. 5. A practical demonstration of the numerical stability of the recurrence relations for the $L^{(4)}$ and $T$ matrices was given in Ref. 6.

## III. ALGORITHMS

Let us divide the integration range $[x',x'']$ into $M$ sectors of length $2h$, $[x',x''] = \Sigma_{p=1}^{M} [x_{2p-2},x_{2p}]$, where $x' = x_0$ and $x'' = x_M$, and consider the boundary value problems (2) and (2a) in the $p$th sector, i.e., replace $[x',x'']$ with $[x_{2p-2},x_{2p}]$ in Eq. (2a), denoting the corresponding solutions by $\psi^{\alpha}_{[p]}$ for $\alpha = +,-,0$. Partitioning the matrices $B(x)$ and $\phi(x)$ within this sector into two parts;

$$Y(x) = Y^{p}_{\text{ref}} + Y^{p}(x) \quad \text{for } Y = B,\phi \quad \text{and for } x \in [x_{2p-2},x_{2p}] , \tag{14}$$

with constant, and diagonal for $Y = B$, reference matrices chosen at the midpoint $x_{2p-1}$;

$$\phi^{p}_{\text{ref}} := \phi(x_{2p-1}) , \tag{14a}$$

$$B^{p}_{\text{ref}} := \text{diag}[B(x_{2p-1})] := (k^{p})^2 , \tag{14b}$$

and, correspondingly, partitioning the operator $D$;

$$D = D^{p}_{\text{ref}} + B^{p} , \tag{15}$$

where

$$D^{p}_{\text{ref}} := \frac{d^2}{dx^2} + B^{p}_{\text{ref}} , \tag{15a}$$

let us specify the sector reference problems:

$$D^{p}_{\text{ref}} \varphi^{\alpha}_{[p]} = \delta_{\alpha,0} \phi^{p}_{\text{ref}} \quad \text{for } \alpha = +,-,0 , \tag{16}$$

$$\varphi^{\pm}_{[p]}(x_{2p-2}) = \begin{cases} I \\ 0 \end{cases}, \quad \varphi^{\pm}_{[p]}(x_{2p}) = \begin{cases} 0 \\ I \end{cases},$$

$$\varphi^{0}_{[p]}(x_{2p-2}) = \varphi^{0}_{[p]}(x_{2p}) = 0 . \tag{16a}$$

Obviously, in terms of the solutions of these problems, $\varphi^{\alpha}_{[p]}$, obtainable analytically, the solutions of the full problems in the sector $p$, $\psi^{\alpha}_{[p]}$, can be expressed

$$\psi^{\alpha}_{[p]} = \varphi^{\alpha}_{[p]} + \chi^{\alpha}_{[p]} \quad \text{for } \alpha = +,-,0 , \tag{17}$$

where

$$\chi^{\alpha}_{[p]} = -G^{0}_{[p]}(B^{p}\psi^{\alpha}_{[p]} - \delta_{\alpha,0}\phi^{p}) , \tag{17a}$$

using the Green's function for the operator $D^{p}_{\text{ref}}$, $G^{0}_{[p]}$, analogous to the Green's function $G^{0}_{x',x''}$ introduced above for the operator $D$. Thus, $G^{0}_{[p]}$ can be evaluated according to the formulas (9) and (9a) after replacing the functions $\psi^{\pm}_{x',x''}$ with the functions $\varphi^{\pm}_{[p]}$. Now, let us introduce sector counterparts of the $J^{\alpha}_{x',x''}$ integrals, the integrals $J^{\alpha}_{[p]}$, $J^{\alpha}_{[p]} = \langle \psi^{\alpha}_{[p]},\phi \rangle$, for $\alpha = +,-,0$, and separate from them the terms which can be evaluated analytically (the first term in the equation below):

$$J^{\alpha}_{[p]} = \langle \varphi^{\alpha}_{[p]},\phi^{p}_{\text{ref}} \rangle + \langle \chi^{\alpha}_{[p]},\phi^{0}_{\text{ref}} \rangle + \langle \psi^{\alpha}_{[p]},\phi^{p} \rangle \quad \text{for } \alpha = +,-,0 . \tag{18}$$

In order to evaluate the remaining terms, the functions $\psi^{\alpha}_{[p]}$ have to be found. With this purpose the integral equations (17) and (17a) are discretized by means of the modified Simpson quadrature formula (cf. Refs. 6, 8, 11, and 16 and Appendix B), giving the following algebraic equations:

$$F^{\alpha}_{[p]}(x_i) = \varphi^{\alpha}_{[p]}(x_i) - \sum_{k=2p-2}^{2p} \omega_k G^{0}_{[p]}(x_i,x_k) q^{p}_{k} \times [B^{p}(x_k)F^{\alpha}_{[p]}(x_k) - \delta_{\alpha,0}\phi^{p}(x_k)] \tag{19}$$

for the functions $F^{\alpha}_{[p]}(x_k)$ related to the functions $\psi^{\alpha}_{[p]}(x_k)$ through the formula

$$F^{\alpha}_{[p]}(x_k) := (q^{p}_{k})^{-1}\psi^{\alpha}_{[p]}(x_k) - \delta_{\alpha,0}\gamma_k\phi^{p}(x_k) \quad \text{for } \alpha = +,-,0 \tag{19a}$$

where

$$q^{p}_{k} := [I + \gamma_k B^{p}(x_k)]^{-1} , \tag{19b}$$

and

$$\omega_k = 4h/3 \ (h/3), \quad \gamma_k = h^2/6 \ (0) \quad \text{for odd (even) } k . \tag{19c}$$

However, instead of solving Eqs. (19)–(19c) directly for the functions $\psi^{\alpha}_{[p]}$ it is more profitable to exploit the concept of invariant imbedding once more; this time, in connection with the discrete boundary value problem given by Eq. (19). Namely, breaking up the $p$th sector into half-sectors $[x_l,x_{l+1}]$ with $l = 2p-2, 2p-1$, let us introduce analogous equations for half-sector functions $F^{\alpha}$, $F^{\alpha}_{l,l+1}(x_i)$ with $l = 2p-2, 2p-1$;

$$F^{\alpha}_{l,l+1}(x_i) = \varphi^{i}_{l,l+1}(x_i) - \sum_{k=l}^{l+1} \tilde{\omega}_k G^{0}_{l,l+1}(x_i,x_k) q^{p}_{k} \times [B^{p}(x_k)F^{\alpha}_{l,l+1}(x_k) - \delta_{\alpha,0}\phi^{p}(x_k)] , \tag{20}$$

where $\tilde{\omega}_k = 2h/3 \ (h/3)$ for odd (even) $k$; the functions $\varphi^{\alpha}_{l,l+1}$ and $G^{0}_{l,l+1}$ are defined analogously to the sector functions $\varphi^{\alpha}_{[p]}$ and $G^{0}_{[p]}$, respectively. [This means that the boundary conditions (16a) are imposed at the points $x_l$ and $x_{l+1}$ in the case of the functions $\varphi^{\alpha}_{l,l+1}$. The reference matrices $B^{p}_{\text{ref}}$ and $\phi^{p}_{\text{ref}}$ are kept the same, however, in both half-sectors.]

Preserving analogy with the relation (19a), let us introduce also half-sector functions $\psi^{\alpha}$, $\psi^{\alpha}_{l,l+1}(x_i)$:

$$\psi^{\alpha}_{l,l+1}(x_i) := q^{p}_{i}[F^{\alpha}_{l,l+1}(x_i) + \gamma_i\delta_{\alpha,0}\phi^{p}(x_i)] := q^{p}_{i}\varphi^{\alpha}_{l,l+1}(x_i) + \chi^{\alpha}_{l,l+1}(x_i) , \tag{21}$$

which assume the following values:

$$\psi^{\pm}_{l,l+1}(x_l) = \begin{cases} q^{p}_{l} \\ 0 \end{cases}, \quad \psi^{\pm}_{l,l+1}(x_{l+1}) = \begin{cases} 0 \\ q^{p}_{l+1} \end{cases}, \tag{21a}$$

$$\psi^{0}_{l,l+1}(x_i) = \chi^{0}_{l,l+1}(x_i) = \gamma_i q^{p}_{i}\phi^{p}(x_i) ,$$

$$\chi^{+}_{l,l+1}(x_i) = \chi^{-}_{l,l+1}(x_i) = 0 \quad \text{for } i = l,l+1 .$$

In connection with the above half-sector equations, the effective half-sector $L$ matrices (cf. Ref. 8);

$$L_{l,l+1} := \begin{pmatrix} \dot{F}^{+}_{l,l+1}(x_l) & \dot{F}^{-}_{l,l+1}(x_l) \\ \dot{F}^{+}_{l,l+1}(x_{l+1}) & \dot{F}^{-}_{l,l+1}(x_{l+1}) \end{pmatrix}, \tag{22}$$

and the following half-sector integrals come into consideration:

$$J^{\alpha}_{l,l+1} := \langle \varphi^{\alpha}_{l,l+1}, \phi^{p}_{\mathrm{ref}} \rangle + \{ \chi^{\alpha}_{l,l+1}, \phi^{p}_{\mathrm{ref}} \} + \{ \psi^{\alpha}_{l,l+1}, \phi^{p} \} \quad \text{for } \alpha = +, -, 0, \tag{23}$$

where

$$\{ Y_{l,l+1}, Z \} := \sum_{k=l}^{l+1} \tilde{\omega}_k Y^{T}_{l,l+1}(x_k) Z(x_k) .$$

The following formulas can be derived for these quantities:

$$L_{l,l+1} = \begin{pmatrix} -(l^p - hS^p_l)/h & s^p/h \\ -s^p/h & (l^p - hS^p_{l+1})/h \end{pmatrix} \quad \text{for } l = 2p-2, 2p-1, \tag{22a}$$

where

$$S^p_l = \tilde{\omega}_l q^p_l B^p_l \quad [B^p_l := B^p(x_l)], \tag{22b}$$

$$s^p = \begin{cases} h|k^p|/\sin(h|k^p|) & \text{if } (k^p)^2 > 0 \\ h|k^p|/\sinh(h|k^p|) & \text{if } (k^p)^2 < 0 \end{cases}, \tag{22c}$$

$$l^p = \begin{cases} h|k^p|\cot(h|k^p|) & \text{if } (k^p)^2 > 0 \\ h|k^p|\coth(h|k^p|) & \text{if } (k^p)^2 < 0 \end{cases}, \tag{22d}$$

$$J^{+}_{l,l+1} = b^p/h + \tilde{\omega}_l q^p_l \phi^p_l \quad [\phi^p_l := \phi^p(x_l)], \tag{23a}$$

$$J^{-}_{l,l+1} = b^p/h + \tilde{\omega}_{l+1} q^p_{l+1} \phi^p_{l+1}, \tag{23b}$$

$$J^{0}_{l,l+1} = e^p/h + \sum_{k=l}^{l+1} \tilde{\omega}_k \gamma_k (\phi^p_k)^T q^p_k \phi_k \quad \text{for } l = 2p-2, 2p-1, \tag{23c}$$

where

$$b^p := h\langle \varphi^{+}_{l,l+1}, \phi^p_{\mathrm{ref}} \rangle = h\langle \varphi^{-}_{l,l+1}, \phi^p_{\mathrm{ref}} \rangle = (s^p - l^p)/(k^p)^2 \phi^p_{\mathrm{ref}}, \tag{23d}$$

$$e^p := h\langle \varphi^{0}_{l,l+1}, \phi^{0}_{\mathrm{ref}} \rangle = (\phi^p_{\mathrm{ref}})^T [2(l^p - s^p) + (hk^p)^2]/|k^p|^4 \phi^p_{\mathrm{ref}} . \tag{23e}$$

Use has been made in the derivation of the explicit form of the functions $\varphi^{\pm}_{l,l+1}(x)$:

$$\varphi^{-}_{l,l+1}(x) = \sin[|k^p|(x - x_l)]/\sin(h|k^p|), \tag{24a}$$

$$\varphi^{+}_{l,l+1}(x) = -\sin[|k^p|(x - x_{l+1})]/\sin(h|k^p|) \quad \text{if } (k^p)^2 > 0 \tag{24b}$$

[the hyperbolic sines appear when $(k^p)^2 < 0$], and of the function $\varphi^{0}_{l,l+1}(x)$:

$$\varphi^{0}_{l,l+1}(x) = \int_{x_l}^{x_{l+1}} G^{0}_{l,l+1}(x,y)\, dy \cdot \phi^p_{\mathrm{ref}}, \tag{24c}$$

where

$$G^{0}_{l,l+1} = (W[\varphi^{-}_{l,l+1}, \varphi^{+}_{l,l+1}])^{-1} \varphi^{-}_{l,l+1}(x_<) \varphi^{+}_{l,l+1}(x_>),$$
$$x_<(x_>) := \min(\max)(x,y) .$$

The expressions (22a)–(22d) for the half-sector $L$ propagator were obtained for the first time by Manolopoulos[10] as the result of his idea to implement the constant reference potentials (the $B^p_{\mathrm{ref}}$ matrices in the present notation) into the original log-derivative method. A straightforward extension of this idea is the use of the constant reference matrices $\phi^p_{\mathrm{ref}}$ which has led to the expressions (23a)–(23e) for the half-sector $J$ integrals. Obviously, setting to zero all the reference matrices one gets the purely approximate-solution-type expressions which have been derived previously for all the quantities considered[6,8] except for the $J^0$ integral.

Having derived the formulas for the half-sector $J$ integrals one can insert them into the recurrence relations (12a)–(12c) and obtain the corresponding formulas for the sector integrals. Obviously, to get the values of the $J$ integrals over the desired integration range one has to "add" the integrals evaluated in subsequent sectors of this range, also using the relations (12a)–(12d). An alternate and more efficient way is to perform the "addition" by half-sectors. This way has been assumed in all the log-derivative algorithms constructed so far and is assumed also in the algorithms to be given below. According as the reference matrices can be introduced only into the homogeneous equations or also into the inhomogeneity terms, the following two hybrid approximate-solution approximate-potential versions of the log-derivative method for calculating the $J$ integrals are constructed on the basis of the formulas (22a)–(22d) and (23a)–(23e):

(1) (fully) hybrid version corresponding to the choice: $B^p_{\mathrm{ref}} \neq 0$ and $\phi^p_{\mathrm{ref}} \neq 0$ in all sectors, i.e., for $p = 1, 2, \ldots, M$;

(2) "half-hybrid" version in which $B^p_{\mathrm{ref}} \neq 0$ but $\phi^p_{\mathrm{ref}} = 0$ for $p = 1, 2, \ldots, M$.

To write the algorithms for both cases in possibly concise forms, let us introduce the following working quantities:

$$z_l := hL^{(4)}_{0,l} + l^p - hS^p_l, \tag{25a}$$

$$t_l := h(J^{-}_{0,l} + \tilde{\omega}_l q^p_l \phi^p_l) + b^p, \tag{25b}$$

$$j_l := h[J^{0}_{0,l} + \tilde{\omega}_l \gamma_l (\phi^p_l)^T q^p_l \phi_l] + e^p \quad \text{for } l = 2p-1, \tag{25c}$$

and

$$\tilde{z}_l := h(L^{(4)}_{0,l} - \tilde{\omega}_l B_l), \tag{25d}$$

$$\tilde{t}_l := h(J^{-}_{0,l} + \tilde{\omega}_l \phi_l), \tag{25e}$$

$$j_l := hJ^{0}_{0,l} \quad \text{for } l = 2p, \quad p = 1,2,\ldots,M . \tag{25f}$$

In the fully hybrid case the matrices $\phi^p_l [= \phi^p(x_l)]$ vanish at points $x_{2p-1}$ [cf. Eqs. (14) and (14a)]. The algorithm in this case reads:

(i) For the log-derivative matrix $L^{(4)}_{x',x''} \approx L^{(4)}_{0,2M}$:

$$\tilde{z}_0 = C \quad \text{(a constant diagonal matrix, } C \gg I),$$

$$\left.\begin{aligned} z_l &= 2l^p - 8 + g^p_l - s^p z^{-1}_{l-1} s^p \\ &\text{where } z_{l-1} = \tilde{z}_{l-1} + a^p \end{aligned}\right\} \quad \text{for } l = 2p-1,$$

$$\tilde{z}_l = a^p - 2h^2/3B_l - s^p z^{-1}_{l-1} s^p \quad \text{for } l = 2p$$

$$L^{(4)}_{0,2M} = (\tilde{z}_{2M} + h^2/3B_{2M})/h .$$

(ii) For the integral $J^{-}_{x',x''} \approx J^{-}_{0,2M}$

$$\tilde{t}_0 = h^2/3\phi_0 ,$$

$$\left.\begin{aligned} t_l &= 2b^p + s^p z_{l-1}^{-1} t_{l-1} \\ &\text{where } t_{l-1} = \tilde{t}_{l-1} + c^p \end{aligned}\right\} \quad \text{for } l = 2p-1 ,$$

$$\tilde{t}_l = c^p + 2h^2/3\phi_l + s^p z_{l-1}^{-1} t_{l-1} \quad \text{for } l = 2p ,$$

$$J_{0,2M}^{-} = (\tilde{t}_{2M} - h^2/3\phi_{2M})/h .$$

(iii) For the integral $J_{x',x''}^0 \approx J_{0,2M}^0$:

$$j_0 = 0 ,$$

$$j_l = j_{l-1} - t_{l-1}^T z_{l-1}^{-1} t_{l-1} + \begin{cases} 2e^p & \text{for } l = 2p-1 \\ 0 & \text{for } l = 2p \end{cases} ,$$

$$J_{0,2M}^0 = j_{2M}/h \quad p = 1,2,\ldots,M .$$

The quantities used above and not defined so far are

$$g_l^p := [0.125 + h^2/48(B_l - B_{\text{ref}}^p)]^{-1} \quad (= 8q_l^p) ,$$

$$a^p := l^p + h^2/3B_{\text{ref}}^p ,$$

$$c^p := b^p - h^2/3\phi_{\text{ref}}^p .$$

In the half-hybrid case the matrices $b^p$ and $e^p$ are zero and $\phi_k^p = \phi_k$ in the formulas (23a)–(23c) and (25a)–(25c). Since $\gamma_l = 0$ and $q_l^p = I$ for even $l$ [cf. Eqs. (19b) and (19c)] it suffices to use only one set of auxiliary quantities related to the $J_{0,l}^{\alpha}$ integrals for both even and odd values of $l$:

$$t_l := h(J_{0,l}^{-} + \tilde{\omega}_l q_l^p \phi_l) , \tag{26a}$$

$$j_l := h\,[J_{0,l}^0 + \tilde{\omega}_l \gamma_l (\phi_l)^T q_l^p \phi_l]$$

$$\text{for } l = 2p-1, 2p \text{ and } p = 1,\ldots,M . \tag{26b}$$

Obviously, the part of the hybrid algorithm concerning evaluation of the log-derivative matrix does not change; the remaining parts reduce in the half-hybrid case to the following forms:

(ii)′

$$t_0 = h^2/3\phi_0 ,$$

$$t_l = s^p z_{l-1}^{-1} t_{l-1} + \begin{cases} h^2/6g_l^p\phi_l & \text{for } l = 2p-1 \\ 2h^2/3\phi_l & \text{for } l = 2p \end{cases} ,$$

$$J_{0,2M}^{-} = (t_{2M} - h^2/3\phi_{2M})/h .$$

(iii)′

$$j_0 = 0 ,$$

$$j_l = j_{l-1} - t_{l-1}^T z_{l-1}^{-1} t_{l-1} + \begin{cases} h^4/36\phi_l^T g_l \phi_l & \text{for } l = 2p-1 \\ 0 & \text{for } l = 2p \end{cases} ,$$

$$J_{0,2M}^0 = j_{2M}/h , \quad p = 1,2,\ldots,M .$$

To switch from the half-hybrid case to the purely approximate-solution case one has to set: $s^p = I$, $l^p = I$, $a^p = I$, and $g_l^p \to g_l = (0.125 + h^2/48B_l)^{-1}$ in the formulas (i), (ii)′, and (iii)′. In that way one obtains: the original log-derivative algorithm of Johnson, the extension of this algorithm to the $J^-$ integral derived in Ref. 6 (rederived and tested recently in Ref. 11), and the most direct extension of the log-derivative algorithm to the $J^0$ integral which is new.

## IV. NUMERICAL TESTS ON A NONADIABATIC MODEL OF THE $H_2$ MOLECULE

In the assumed model, the nuclear motion of $H_2$ in the $B\,^1\Sigma_u^+$, $B'\,^1\Sigma_u^+$, and $D\,^1\Pi_u$ electronic states is described by the following $3\times3$ matrix Hamiltonian:

$$\mathbf{H} = \begin{pmatrix} \mathbf{H}^{00} & \mathbf{V}^{0D} \\ \mathbf{V}^{D0} & H^D \end{pmatrix} = -1/(2\mu)\left(I\frac{d}{dx} + \mathbf{A}\right)^2 + \mathbf{V} \tag{27}$$

with the matrices $\mathbf{A}$ and $\mathbf{V}$ having the structures

$$\mathbf{A} = \begin{pmatrix} \mathbf{a} & 0 \\ 0 & 0 \end{pmatrix}, \quad \mathbf{a}^T = -\mathbf{a} , \tag{27a}$$

$$\mathbf{V} = \begin{pmatrix} \mathbf{V}^{00} & \mathbf{V}^{0D} \\ (\mathbf{V}^{0D})^T & V^D \end{pmatrix},$$

$$(\mathbf{V}^{00})_{i,j} = \delta_{i,j} V^i, (\mathbf{V}^{0D})_i = V_{i,D} \quad \text{for } i = B,B' . \tag{27b}$$

Consistently, the structures of the Hamiltonians $\mathbf{H}^{00}$ and $H^D$ are

$$(\mathbf{H}^{00})_{i,j} = \delta_{i,j} H^i - 1/(2\mu)\left[2\mathbf{a}_{i,j}\frac{d}{dx} + (\mathbf{a}^2)_{i,j} + \dot{\mathbf{a}}_{i,j}\right]$$

$$\text{for } i,j = B,B' , \tag{27c}$$

$$H^i = -1/(2\mu)\frac{d^2}{dx^2} + V^i \quad \text{for } i = B,B',D . \tag{27d}$$

The respective adiabatic potentials and nonadiabatic couplings are assumed in the form of the following functions of the internuclear coordinate with parameters as listed in Table I:

$$V^i(x) = D_i\{1 - \exp[\beta_i(x - x_i^{\min})]\} + V_i^{\min}$$

$$\text{for } i = B,B',D, \tag{27e}$$

$$V_{i,D}(x) = a_i \exp(-\alpha_i x)/(2\mu x^2) \quad \text{for } i = B,B' , \tag{27f}$$

$$[\mathbf{a}(x)]_{B,B'} = cx^2(x-d)\exp[-g(x-x_0)^2] . \tag{27g}$$

Evidently, the model involves some approximations rather

TABLE I. Parameters[a] of the model of the $H_2$ molecule.

| Adiabatic potentials | | | | |
|---|---|---|---|---|
| State | $V^{\min}$ | $D$ | $x^{\min}$ | $\beta$ |
| $X$ | −1.174 476 | 0.174 475 | 1.400 | 1.027 |
| $B$ | −0.756 68 | 0.131 68 | 2.425 | 0.354 |
| $B'$ | −0.665 7575 | 0.040 7575 | 2.080 | 0.913 |
| $B''$[b] | −0.67 | 0.045 | 2.1 | 0.9 |
| $D$ | −0.655 314 | 0.099 760 | 1.984 | 0.687 |
| $D$[b] | −0.65 | 0.1 | 2.0 | 0.7 |

| Nonadiabatic couplings | | | Transition moments | |
|---|---|---|---|---|
| States | $a$ | $\alpha$ | States | $\gamma$ |
| $D$–$B'$ | 8.0 | 0.8 | $X$–$B$ | 0.4 |
| $D$–$B$ | 1.0 | 0.8 | $X$–$B'$ | 0.3 |
| | | | $X$–$D$ | 0.2 |
| $B$–$B'$ | $c = 0.0005$ | $d = 4.5$ | | |
| | $g = 0.1$ | $x = 9.0$ | $\mu = 918.0764$ | |
| | | | 900.0[b] | |

[a] All parameters are given in a.u.

[b] Parameters used in the tests of Sec. IV B.

crude from a physical point of view, like omission of the centrifugal term or suppression of the total angular momentum dependent factor from the coupling (rotational in origin) of the $D$ state with the $B$ and $B'$ states, denoted collectively by the "0" superscript. Moreover, the Morse oscillators used for the adiabatic potentials reproduce only crudely the true *ab initio* potentials, especially in the case of the $B$ state. These approximations, however, are not essential for modeling the computational requirements connected with determination of continuum or bound rovibrational states of $H_2$ in the realistic nonadiabatic approach.

### A. Predissociation of the $D$ state by photon impact

The states of relevance in description of predissociation of the $D$ state of $H_2$ by photon impact are:

(i) the (energy normalized) scattering states, $\mathbf{F}^B$ and $\mathbf{F}^{B'}$, of the Hamiltonian $\mathbf{H}$ in the range of energy $E$ between the $D$ state and the $B$, $B'$ states dissociation limits, i.e., for $E_B^\infty (= E_{B'}^\infty) < E < E_D^\infty$, where $E_i^\infty = D_i + V_i^{\min}$, with asymptotic behavior of outgoing waves ($s$ waves in the present model);

$$(E - \mathbf{H})\mathbf{F} = 0, \quad \mathbf{F} := (\mathbf{F}^B, \mathbf{F}^{B'}) , \tag{28}$$

$$\mathbf{F}(x_0 \approx 0) = 0 , \tag{28a}$$

$$\mathbf{F}(x) = i/2(2\mu/\pi)^{1/2}[O^-(x) - O^+(x)\mathbf{S}] \quad \text{for } x \geqslant x_\infty , \tag{28b}$$

where

$$[O^\pm(x)]_{i,j} = \delta_{i,j} \exp(\pm ik_i x)/(|k_i|)^{1/2} , \tag{28c}$$

$$k_i = [2\mu(E - E_i^\infty)]^{1/2} \quad \text{for } i = B, B', D \quad (k_D = i|k_D|) . \tag{28d}$$

(ii) The bound states $\chi_v^i$ with $i = D, X$, of the Hamiltonian $H^D$ and of the Hamiltonian $H^X$ defined analogously [i.e., by Eqs. (27d) and (27e)] for the ground $X\,{}^1\Sigma_g^+$ state of $H_2$:

$$H^i \chi_v^i = \epsilon_v^i \chi_v^i \quad \text{for } i = D, X . \tag{29}$$

The cross section for transition of $H_2$ from the bound state $\chi_{v'=0}^X$ into the continuum $\mathbf{F}^B$ and $\mathbf{F}^{B'}$ states by weak photon-matter interaction simulated in the present model by the following matrix operator $\mathbf{M}$:

$$\mathbf{M} = \begin{pmatrix} \mathbf{M}^{0X} \\ M_{D,X} \end{pmatrix}, \quad \mathbf{M}^{0X} = \begin{pmatrix} M_{B,X} \\ M_{B',X} \end{pmatrix}, \tag{30}$$

where

$$M_{i,X} = \exp(-\gamma_i x) \quad \text{for } i = B, B', D \quad (\gamma_i \text{ are also given in Table I}) \tag{30a}$$

is proportional to the quantity

$$\sigma(E) := (E - \epsilon_{v'=0}^X)\mathbf{m}\mathbf{m}^\dagger , \tag{31}$$

where

$$\mathbf{m} := \langle \mathbf{M}\chi_{v'=0}^X, \mathbf{F} \rangle . \tag{31a}$$

(The dagger denotes hereafter Hermitian conjugate). The $D$-state predissociation manifests itself in a peaked structure of this quantity as a function of energy. The peaks [called the $D(v) \leftarrow X(v' = 0)$ resonances below] occur in vicinity of the adiabatic levels $\epsilon_v^0$ with $v \geqslant 3$ and reveal the asymmetric Fano profiles[17];

$$\sigma(e) = \sigma_b + \sigma_a (q + e)^2/(1 + e^2) , \tag{32}$$

where

$$e := 2(E - E_{\text{res}})/\Gamma . \tag{32a}$$

Numerical determination of the parameters of these profiles: $E_{\text{res}}, \Gamma, q, \sigma_a, \sigma_b$, is a task on which the new algorithms will be tested here. Both approaches to determination of the resonance profile parameters employed in Ref. 12: the perturbative configuration mixing (CM) approach of Fano[17] and the more rigorous lifetime (LT) matrix[18] approach, will be exploited in the tests.

In the CM approach, the profile parameters of a $D(v) \leftarrow X(v' = 0)$ resonance are determined according to the formulas

$$E_{\text{res}} = \epsilon_v^D + E_{\text{shift}}, \quad E_{\text{shift}} = \mathcal{J}_{D,D}^R , \tag{33a}$$

$$\Gamma = 2\mathcal{J}_{D,D}^I , \tag{33b}$$

$$q = (\mathcal{J}_{D,X}^R + \mathcal{M}_{D,X})/\mathcal{J}_{D,X}^I , \tag{33c}$$

$$\sigma_a = \omega/\pi(\mathcal{J}_{D,X}^I)^2/\mathcal{J}_{D,D}^I, \quad \omega = E_{\text{res}} - \epsilon_{v'=0}^X , \tag{33d}$$

$$\sigma_b = \sigma_0 - \sigma_a, \quad \sigma_0 = \omega/\pi \mathcal{J}_{X,X}^I , \tag{33e}$$

which involve the following integrals:

$$\mathcal{M}_{D,X} := \langle \chi_V^D, M_{D,X}\chi_{v'=0}^X \rangle , \tag{34}$$

$$\mathcal{J} := \langle \varphi, \mathcal{G}^+ \varphi \rangle = \begin{pmatrix} \mathcal{J}_{X,X} & \mathcal{J}_{X,D} \\ \mathcal{J}_{D,X} & \mathcal{J}_{D,D} \end{pmatrix}, \tag{35}$$

$$\mathcal{J}_{i,j}^R := \text{Re}(\mathcal{J}_{i,j}), \quad \mathcal{J}_{i,j}^I := -\text{Im}(\mathcal{J}_{i,j}) \quad \text{for } i,j = X, D ,$$

with

$$\varphi := (\varphi^X, \varphi^D) := (\mathbf{M}^{0X}\chi_{v'=0}^X, \mathbf{V}^{0D}\chi_v^D) , \tag{35a}$$

and with $\mathcal{G}^+$ being the outgoing-wave Green's function of the operator $\mathcal{D}, \mathcal{D} := 2\mu(E - \mathbf{H}^{00})$, at $E = E_{\text{res}}$;

$$1/(2\mu)\mathcal{D}\mathcal{G}^+(x,y) = I\delta(x - y) , \tag{36}$$

$$\mathcal{G}^+(x_0, y) = 0, \quad \mathcal{G}^+(x,y) = O^+(x) g^T(y) \quad \text{for } x \geqslant x_\infty . \tag{36a}$$

Two analytical steps are necessary in order to make the algorithms of the previous section applicable to these formulas. Firstly, the integral $\mathcal{J}$ is related to the integrals involving $\mathcal{G}^0$ counterpart of the function $\mathcal{G}^+$, i.e., the Green's function which satisfies Eq. (36) and the boundary conditions:

$$\mathcal{G}^0(x_0, y) = \mathcal{G}^0(x_\infty, y) = 0. \tag{36b}$$

The respective relation reads [cf. Eqs. (11) and (11a)]

$$\mathcal{J} = 2\mu(\mathcal{J}_{x_0,x_\infty}^-)^T(L_0 - \mathcal{L}_{x_0,x_\infty})^{-1}\mathcal{J}_{x_0,x_\infty}^- + \langle \varphi, \mathcal{G}^0 \varphi \rangle , \tag{37}$$

where

$$\mathcal{J}_{x_0,x_\infty}^\alpha := \langle f_{x_0,x_\infty}^\alpha, \varphi \rangle := ((\mathcal{J}_{x_0,x_\infty}^\alpha)^X, (\mathcal{J}_{x_0,x_\infty}^\alpha)^D) \quad \text{for } \alpha = -0, \tag{37a}$$

$$\mathcal{L}_{x_0,x_\infty} := f_{x_0,x_\infty}(x_\infty) , \tag{37b}$$

$$\langle \varphi, \mathcal{G}^0 \varphi \rangle = 2\mu \mathcal{J}_{x_0,x_\infty}^0 , \tag{37c}$$

and $f_{x_0,x_\infty}^\alpha$ are solutions of the equations

$$\mathscr{D}\mathscr{f}^{\alpha}_{x_0,x_\infty} = \delta_{\alpha,0}\varphi \quad \text{for} \quad \alpha = -0, \tag{38}$$

satisfying the boundary conditions (2a) in the interval $[x',x''] = [x_0,x_\infty]$. Secondly, the boundary value problems for the functions $\mathscr{f}^{\alpha}_{x_0,x_\infty}$ are converted to the form of Eqs. (1) and (2);

$$\mathscr{T}^T\mathscr{D}\mathscr{T} = I\frac{d^2}{dx^2} + B(x), \tag{39}$$

where

$$B(x) = \mathscr{T}^T(x)\mathbf{V}^{00}(x)\mathscr{T}(x), \tag{39a}$$

$$\phi(x) = \mathscr{T}^T(x)\varphi(x), \tag{40}$$

by means of the orthogonal transformation $\mathscr{T}(x)$:

$$\left(I\frac{d}{dx} + \mathbf{a}\right)\mathscr{T}(x) = 0, \quad \mathscr{T}(x_0) = I, \tag{41}$$

giving the relations

$$\mathscr{L}_{x_0,x_\infty} = \mathscr{T}(x_\infty)L^{(4)}_{x_0,x_\infty}\mathscr{T}^T(x_\infty), \tag{42a}$$

$$\mathscr{J}^{-}_{x_0,x_\infty} = \mathscr{T}(x_\infty)J^{-}_{x_0,x_\infty}, \tag{42b}$$

$$\mathscr{J}^{0}_{x_0,x_\infty} = J^{0}_{x_0,x_\infty}. \tag{42c}$$

The parameter $\sigma_0$, being the open-channel counterpart of the cross section $\sigma$, can be evaluated also in another way using formulas analogous to the formulas (31) and (31a):

$$\sigma_0 = (E_{\text{res}} - \epsilon^{x}_{v'=0})\mathbf{m}^0(\mathbf{m}^0)^\dagger, \tag{43}$$

where

$$\mathbf{m}^0 := \langle \mathbf{M}^{0x}\chi^{x}_{v'=0}, \mathbf{f}\rangle \tag{43a}$$

$$= i/2(2\mu/\pi)^{1/2}(\mathscr{J}^{-}_{x_0,x_\infty})^x[O^-(x_\infty) - O^+(x_\infty)\mathbf{s}]. \tag{43b}$$

$\mathbf{f}$ is the solution of the problem (28)–(28d) after replacing the operator $\mathbf{H}$ with its $\mathbf{H}^{00}$ part and $\mathbf{s}$ is the corresponding scattering $S$ matrix:

$$\mathbf{s} = [\dot{O}^+(x_\infty) - \mathscr{L}_{x_0,x_\infty}O^+(x_\infty)]^{-1} \times [\dot{O}^-(x_\infty) - \mathscr{L}_{x_0,x_\infty}O^-(x_\infty)]. \tag{44}$$

In the LT approach, the solutions of the full problem (28)–(28d) are generated numerically and the resonance profile parameters are determined by analyzing variation with energy of the matrix $\mathbf{S}$ and of the cross section $\sigma$ [evaluated according to the formulas (31) and (31a)]. The $E_{\text{res}}$ parameter is determined first, as the position of maximum of the maximal eigenvalue, $Q_{\max}$, of the lifetime matrix $\mathbf{Q}$ in the vicinity of a given $\epsilon^D_v$ level;

$$\mathbf{Q}(E) := i\mathbf{S}(E)\frac{d}{dE}\mathbf{S}^\dagger(E). \tag{45}$$

Simultaneously, the $\Gamma$ parameter is obtained:

$$\Gamma = 4/Q_{\max}(E_{\text{res}}). \tag{46}$$

Then, the cross section $\sigma_{\text{res}} := \sigma(E_{\text{res}})$ and its derivative $\sigma'_{\text{res}} := d\sigma_{\text{res}}/dE$ at the resonance center are calculated, and the minimum value of $\sigma$ within the resonance profile, $\sigma_{\min}$, is found, giving the three remaining parameters:

$$\sigma_b = \sigma_{\min}, \quad q = 4(\sigma_{\text{res}} - \sigma_{\min})/(\Gamma\sigma'_{\text{res}}),$$
$$\text{and} \quad \sigma_a = \sigma'_{\text{res}}\Gamma/(4q). \tag{47}$$

Obviously, the log-derivative algorithms can be applied to evaluation of the necessary matrices $\mathbf{S}$ and of the cross section $\sigma$ in the analogous way as to evaluation of the matrices $\mathbf{s}$ [cf. Eq. (44)] and of the cross section $\sigma_0$ [cf. Eq. (43b)], respectively. It should be stressed, however, that achieving sufficiently high accuracy in the case of the former quantities is much harder than in the case of the latter quantities varying smoothly with energy in the resonance regions.

Accuracy of the new algorithms in the predissociation calculations will be demonstrated on two $D(v) \leftarrow X(v'=0)$ resonances, for $v=3$ and $v=6$, which represent cases of small and large relative kinetic energies of the receding atoms, respectively. The positions of these resonances above the $E^{\infty}_{B}$ ($= E^{\infty}_{B'}$) threshold and the parameters of their profiles in the cross section $\sigma$ are given in Table II. In figs. 1(a) and 1(b) are compared: the rms errors of the matrices $\mathbf{S}$:

$$\text{rms error}(\mathbf{S}): = \left(\sum_{i,j=1}^{N_{\text{open}}} |\mathbf{S}_{i,j} - \mathbf{S}^{\text{ref}}_{i,j}|^2\right)^{1/2}/N^2_{\text{open}} \quad (N_{\text{open}} = 2) \tag{48}$$

and the relative errors of cross section $\sigma$ [cf. Eqs. (31) and

TABLE II. Profile parameters[a] of two $D(v) \leftarrow X(v'=0)$ resonances[b] obtained in the LT and in the CM approaches[c]

| | $v=3$ | | $v=6$ | |
|---|---|---|---|---|
| | LT | CM | LT | CM |
| $E_{\text{shift}}$ | 0.506 4 ( − 5)[d] | 0.503 9 ( − 5) | 0.262 1 ( − 5) | 0.260 1 ( − 5) |
| $\Gamma$ | 0.208 4 ( − 4) | 0.203 3 ( − 4) | 0.256 6 ( − 4) | 0.254 7 ( − 4) |
| $q$ | 0.213 79 ( + 2) | 0.215 06 ( + 2) | 0.162 77 ( + 2) | 0.167 09 ( + 2) |
| $\sigma_a$ | 0.384 1 ( + 1) | 0.379 1 ( + 1) | 0.155 3 ( + 1) | 0.147 1 ( + 1) |
| $\sigma_b$ | 0.081 | 0.081 | 0.389 ( − 2) | 0.398 ( − 2) |
| $\sigma_0$ | | 0.387 2 ( + 1) | | 0.147 5 ( + 1) |
| $E_{\text{res}}$ | − 0.623 006 515 | − 0.623 006 54 | − 0.600 334 97 | − 0.600 334 99 |
| $\sigma_{\text{res}}$ | 0.175 551 ( + 4) | 0.175 345 ( + 4) | 0.411 50 ( + 3) | 0.410 69 ( + 3) |

[a] All parameters except for the dimensionless parameter $q$ are given in appropriate atomic units.
[b] $\epsilon^D_{v=3} = -0.623\,011\,579$ a.u., $\epsilon^D_{v=6} = -0.600\,337\,591$ a.u.; $E^{\infty}_{B} = -0.625$ a.u.
[c] The values listed here were obtained by the "half-hybrid" algorithm using the step $h = 0.005$ a.u. in the range $[x_0, x_\infty] = [0.001, 50.0]$ a.u.
[d] The numbers in parentheses denote powers of 10.

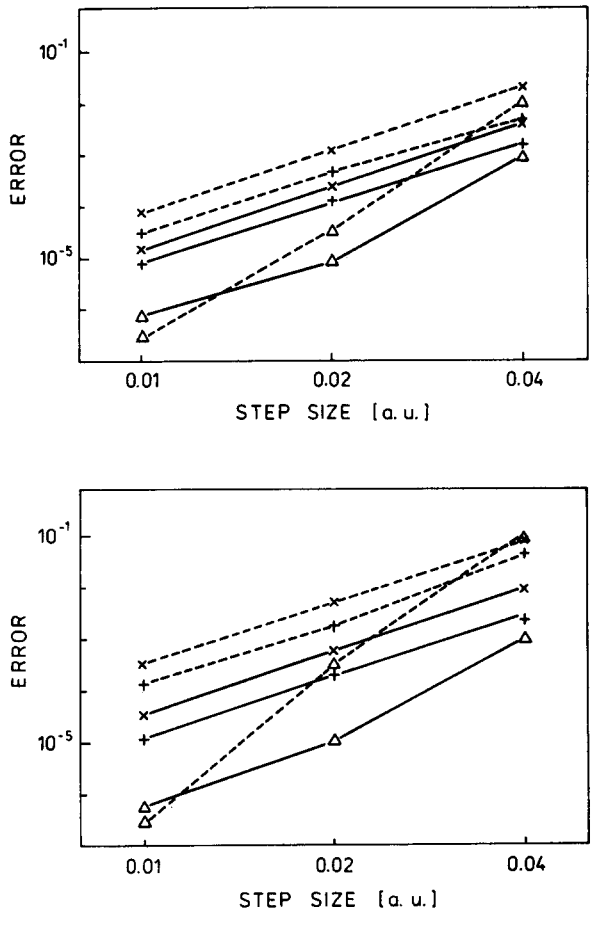


FIG. 1. (a) Errors of results generated (in the LT approach) by the half-hybrid (–) and by the nonhybrid (- - -) log-derivative algorithms at energy equal to $E_{res}$ value of $D(v=3) \leftarrow X(v'=0)$ resonance (see Table II); (×) rms error (S); ( + ) rel. error ($\sigma$); (△) rel. error ($\Gamma$). (b) Same as in (a) but for $E_{res}$ energy of $D(v=6) \leftarrow X(v'=0)$ resonance.

(31a)] and of the profile width $\Gamma$ [cf. Eq. (46)]; rel. error $x := |1 - x/x^{ref}|$ for $x = \sigma$, $\Gamma$, which were encountered in the LT calculations at $E_{res}$ energies of the two resonances by the nonhybrid and the by the half-hybrid algorithms with three different step sizes, $h$. The results of the half-hybrid algorithm with the step size $h = 0.005$ a.u., listed in Table II, were used as reference values in error evaluations. It is demonstrated that the rms errors of the matrices S generated by both versions of the log-derivative algorithm were strictly proportional to $h^4$ (cf. Ref. 10); the same feature was revealed by the errors of $\sigma$. The errors of both quantities were smaller, ten times in the $v = 6$ case and approximately four times in the $v = 3$ case, when the hybrid algorithms were used. (No significant differences in errors were encountered between the results obtained by the half-hybrid and the fully hybrid versions in the cases shown in Fig. 1.) Accuracy of the matrices S is certainly the basic factor influencing accuracy of the resonance widths $\Gamma$ and also of the resonance positions $E_{res}$ determined with the LT approach. The actual errors of these quantities, for the $\Gamma$ quantity shown in Fig. 1, account additionally for inaccuracies of numerical differentiation involved in the evaluation of the lifetime matrix Q [cf. Eq. (45)];

$$\mathbf{Q}(E) \approx i/(4dE)(\mathbf{S}_+ + \mathbf{S}_-)(\mathbf{S}_+ - \mathbf{S}_-)^+, \tag{49}$$

where

$$\mathbf{S}_\pm := \mathbf{S}(E \pm dE).$$

(The value $dE = 10^{-9}$ a.u. was used in all cases in Fig. 1.) Except for the calculations with the small step size $h = 0.01$ a.u. the results for the $\Gamma$ parameter yielded by the hybrid algorithms were definitely more accurate than the nonhybrid results.

Further test of the new algorithms provide the calculations of the resonance profile parameters in the CM approach, reported in Table III. Both the $J^-$- and the $J^0$-type integrals, involving the strongly localized $\chi^X_{v=0}$ and the less localized $\chi^D_{v=3,6}$-bound state functions, had to be generated in these calculations giving an opportunity to expose some differences in performance between the hybrid and the half-hybrid versions. As shown in Table III, the hybrid algorithms, both the half-hybrid and the fully hybrid versions, give more accurate results than the nonhybrid version for the profile parameters of the $D(v=6) \leftarrow X(v'=0)$ resonance. The superiority of the hybrid algorithms is more or less striking depending on the quantity generated. Though accuracy of the results by the fully hybrid algorithm relative to accuracy of the half-hybrid results changes also from quantity to quantity in the present problem it can be expected that the hybrid version will excell in cases with less rapidly varying bound state functions $\varphi$ [cf. Eq. (35)]. In the CM calculations concerning the low lying $D(v=3) \leftarrow X(v'=0)$ resonance the superiority of the hybrid versions over the nonhybrid version is not as evident as it was in the corresponding LT calculations. The factor which matters here is the lack of a (highly) close channel component in the function f. Accurate treatment of such a component in the function F [cf. Eqs. (28)–(28d)] was decisive for the reduction of error in the LT calculations by the hybrid methods shown in Fig. 1(a). Yet another point to note in Table III is the almost perfect $O(h^4)$ behavior of the errors of all the quantities generated, irrespective of the version of the algorithm used.

TABLE III. Errors of CM profile parameters calculated by the nonhybrid (nH), half-hybrid (hH), and by the hybrid (H) log-derivative algorithms error $x := |1 - x/x^{ref}|/h^4$.[a]

| | | $D(v=3) \leftarrow X(v'=0)$ | | | $D(v=6) \leftarrow X(v'=0)$ | | |
|---|---|---|---|---|---|---|---|
| $x$ | $h$ | nH | hH | H | nH | hH | H |
| $E_{shift}$ | 0.04 | 87.9 | 45.2 | 14.9 | 709.4 | 171.1 | 79.3 |
| | 0.02 | 86.7 | 44.9 | 14.4 | 697.0 | 170.0 | 77.4 |
| $\Gamma$ | 0.04 | 28.8 | 4.8 | 18.7 | 66.3 | 16.5 | 34.4 |
| | 0.02 | 28.6 | 4.9 | 18.7 | 65.3 | 16.6 | 34.5 |
| $q$ | 0.04 | 13.6 | 10.1 | 5.9 | 46.6 | 1.1 | 20.4 |
| | 0.02 | 13.5 | 10.2 | 5.9 | 45.9 | 1.3 | 20.3 |
| $\sigma_a$ | 0.04 | 4.1 | 17.2 | 7.7 | 16.6 | 9.9 | 4.5 |
| | 0.02 | 4.0 | 17.2 | 7.7 | 16.4 | 9.8 | 4.2 |
| $\sigma_0$ | 0.04 | 3.4 | 14.8 | 8.2 | 16.3 | 10.6 | 3.9 |
| | 0.02 | 3.3 | 14.8 | 8.3 | 16.2 | 10.4 | 3.6 |

[a] $x^{ref}$—results by the half-hybrid algorithm with the step $h = 0.005$ a.u., listed in Table II.

### B. Nonadiabatic shifts of energy levels below dissociation limit of the $B$ and $B'$ states

In the range of energy $E$ below the dissociation limit of the $B$ and $B'$ states, i.e., at $E < E^{\infty}_{B'}$ ( $= E^{\infty}_{B}$ ), the only effect of the nonadiabatic interactions between these states and the $D$ state are the shifts of the adiabatic energy levels lying in this range:

$$\epsilon^i_v \to E_{(iv)} = \epsilon^i_v + E^{(iv)}_{\text{shift}}$$
$$\text{for } i = B,B',D,\ v < 3 \text{ if } i = D, \tag{50}$$

to the positions corresponding to energies of bound states of $\mathbf{H}$;

$$(E_j - \mathbf{H})\mathbf{F}^j = 0, \quad j := (i,v), \tag{51}$$

$$\mathbf{F}^j(x_0) = \mathbf{F}^j(x_\infty) = 0. \tag{52}$$

The energy shifts $E^{(Dv)}_{\text{shift}}$ for $v = 0,1,2$ are, of course, quantities completely analogous to the $E_{\text{shift}}$ parameter introduced above for the predissociating $D$-state levels $v \geqslant 3$.

The analogous perturbative formula for these shifts involves only the Green's function $\mathscr{G}^0$ [cf. Eq. (36) and (36b)], at energy $E = E_{(Dv)} = \epsilon^D_v + E^{(Dv)}_{\text{shift}}$, and reads

$$E^{(Dv)}_{\text{shift}} = \langle \mathbf{V}^{0D}\chi^D_v, \mathscr{G}^0\mathbf{V}^{0D}\chi^D_v\rangle = 2\mu(\mathscr{J}^0_{x_0,x_\infty})^D$$
$$\text{for } v = 0,1,2. \tag{52}$$

Like the formulas (33a), (35), and (35a), this formula can be exploited in calculations in an iterative way. At the first iteration step, the right-hand side integrals are evaluated using the 0th order approximation to $E_{\text{shift}}$, $(E_{\text{shift}})^{(0)} = 0$.

There is also a possibility to apply the new algorithms to determination of nonperturbative values of the nonadiabatic bound state energies $E_{(iv)}$. To describe it, let us write the Hamiltonian $\mathbf{H}$ as the sum:

$$\mathbf{H} = \mathbf{H}^{\text{ad}} + \lambda\,\mathbf{H}^{\text{nad}}, \tag{53}$$

with

$$(\mathbf{H}^{\text{ad}})_{ij} := \delta_{i,j}H^i \quad \text{for} \quad i = B,B',D, \tag{53a}$$

and with a parameter $\lambda$ characterizing strength of the nonadiabatic interactions. Now, let us introduce the $\mathscr{G}^0$-type Green's function for the operator $\mathbf{H}$, using the $1/(E - \mathbf{H})$ notation this time, and consider the following integral:

$$T_{(iv)}(E,\lambda) := \langle \varphi^i_v, 1/(E - \mathbf{H}^{\text{ad}} - \lambda\,\mathbf{H}^{\text{nad}})\varphi^i_v\rangle, \tag{54}$$

where

$$(\varphi^i_v)_j := \delta_{i,j}\chi^i_v \quad \text{for} \quad i,j = B,B',D. \tag{54a}$$

(As before, $\chi^i_v$ denotes an eigenfunction of $H^i$). $T_{(iv)}$ is, of course, a $J^0$-type integral in the notation of Sec. II. One can easily establish that energy dependence of this integral in vicinity of an $\epsilon^i_v$ level describes the formula

$$T_{(iv)}(E,\lambda) = c_{(iv)}(\lambda)/(E - E_{(iv)}) + r_{(iv)}(E,\lambda), \tag{55}$$

where $c_{(iv)}$ is a quantity of the order of 1 and $r_{(iv)}$ is a small contribution changing smoothly with energy, in cases of $E_{(iv)}$ being well separated from other eigenvalues of $\mathbf{H}$ at least. Thus, $E_{(iv)}$ can be easily determined as position of the pole of $T_{(iv)}(E,\lambda)$ near the adiabatic level $\epsilon^i_v$. As a better estimation of the pole position, the value of $E_{(iv)}$ determined initially by the perturbative formula (52) can be exploited.

In the numerical tests performed as an illustration to the present subsection the $B$ state was not accounted for. Thus, the respective parts of the Hamiltonian actually used are

$$\mathbf{H}^{\text{ad}} = \begin{pmatrix} H^{B'} & 0 \\ 0 & H^D \end{pmatrix}, \quad \lambda\,\mathbf{H}^{\text{nad}} = \begin{pmatrix} 0 & V_{B'D} \\ V_{B'D} & 0 \end{pmatrix}. \tag{56}$$

[The role of the strength parameter $\lambda$ plays the parameter $a_{B'}$, cf. Eq. (27f).]

In Table IV, a comparison is made of the perturbative and of the nonperturbative $E^{(Dv)}_{\text{shift}}$ values of the $v = 0,1,2$ levels calculated in several cases with different strength of the nonadiabatic interaction $V_{B'D}$. The consistency of the results of both kinds testifies to the adequacy of the above nonperturbative procedure, in application to the present problem at least.

An illustration of performance of the three versions of the log-derivative algorithm in evaluation of the integrals $T_{(iv)}(E,\lambda)$ and in determination of the bound state energies with the aid of these integrals is given in Figs. 2(a) and 2(b) and in Table V. A comparison is also made of these algorithms with the Numerov algorithm (strictly speaking, with the invariant imbedding Numerov-related algorithm presented in Appendix A). Accuracy of numerical results yielded by the algorithms considered is tested most rigorously on the integrals $T_{(iv)}(E,\lambda = 0)$ (since their poles are given analytically in the present model);

$$T_{(iv)}(E,\lambda = 0) = 1/(E - \epsilon^i_v). \tag{57}$$

In Fig. 2 are shown the relative errors of the numerical values of these integrals obtained by the four algorithms in the $D$-state ($i = D$) cases, $v = 3$ and $v = 8$, at energies around the respective poles, $\epsilon^D_{v=3}$ and $\epsilon^D_{v=8}$. Again, the hybrid versions of the log-derivative algorithm appear to be more accurate than the nonhybrid version, especially in the case with the highly lying pole $\epsilon^D_{v=8}$. The errors of the calculations by

TABLE IV. Nonadiabatic shifts[a] $E_{(Dv)} - \epsilon^D_v$ for $v = 0, 1, 2$, obtained with Hamiltonian of Eqs. (53) and (56) for several values of coupling parameter $\lambda$ ( $:= a_{B'}$ ). Comparison of perturbative and nonperturbative results.[b]

| $\lambda$ | $v$ | Perturbative[c] | | | Nonperturbative |
|---|---|---|---|---|---|
| 8.0 | 0 | 0.0170 | 0.0169 | (2) | 0.016 9 |
| | 1 | 0.0177 | 0.0176 | (2) | 0.017 6 |
| | 2 | 0.0760 | 0.0749 | (2) | 0.074 9 |
| 10.0 | 0 | 0.0265 | 0.0264 | (2) | 0.026 35 |
| | 1 | 0.0276 | 0.0274 | (2) | 0.027 35 |
| | 2 | 0.1188 | 0.1161 | (2) | 0.116 0 |
| 12.0 | 0 | 0.0382 | 0.0380 | (2) | 0.037 8 |
| | 1 | 0.0398 | 0.0394 | (2) | 0.039 2 |
| | 2 | 0.1711 | 0.1656 | (3) | 0.165 3 |
| 30.0 | 0 | 0.2389 | 0.2301 | (3) | 0.222 9 |
| | 1 | 0.2487 | 0.2335 | (3) | 0.226 3 |
| | 2 | 1.0693 | 0.8977 | (7) | 0.891 9 |

[a] The shifts are given in $10^{-4}$ a.u.

[b] All results were generated by the half-hybrid algorithm using the step $h = 0.01$ a.u. The integration range $[x_0,x_\infty]$ was [0.001,6.0] a.u. in the $v = 0$, 1 cases and $x_\infty = 20.0$ a.u. in the $v = 2$ cases.

[c] Results by formula (52). In first column are listed results obtained at first step, i.e., at respective adiabatic energies $\epsilon^D_v$: $-0.644\,850\,56$, $-0.634\,960\,07$, $-0.625\,613\,93$ a.u., for $v = 0, 1, 2$; in second column are the results iterated over energy; the number of iterations is given in parentheses.

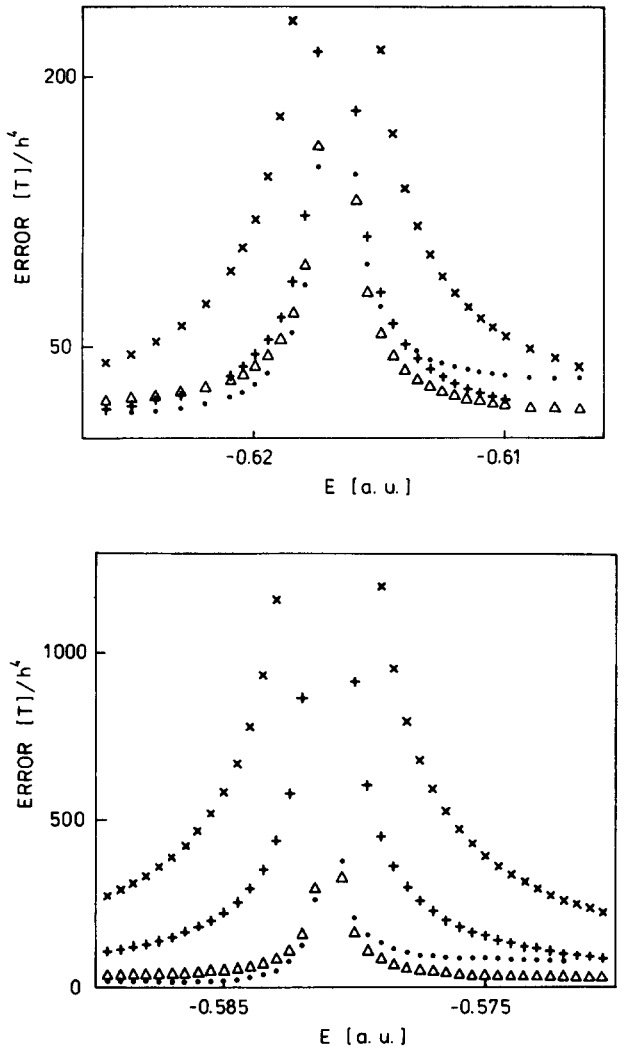


FIG. 2. (a) Errors of $T_{(D,v=3)}$ $(E,\lambda=0)$ integrals generated by the nonhybrid (×), half-hybrid (△), and hybrid (●) log-derivative, and by the Numerov (+) algorithms at energies around the pole $\epsilon^D_{v=3}$. error $(T) := |1 - T/T^{\text{exact}}|$. $T^{\text{exact}}$ values are obtained by the formula (57). The errors are proportional to the fourth power of the step size (see Table V). (b) Same as in (a) but for $T_{(D,v=8)}$ $(E,\lambda=0)$ integrals.

the Numerov algorithm reveal, as expected, similar energy dependence as the errors yielded by the nonhybrid log-derivative algorithm. The latter errors were always found to be larger by a factor of $\sim 2.67$.

One can infer from the above comparison that the poles of the integrals $T_{(Dv)}$ $(E,\lambda=0)$, i.e., the respective bound state energies $\epsilon^D_v$, should be determined most accurately by the hybrid log-derivative algorithms. This is confirmed in Table V where the errors of several $\epsilon^D_v$ energies calculated by the hybrid log-derivative algorithms (the fully hybrid and the half-hybrid versions give exactly the same results here) are shown to be smaller than the errors of the nonhybrid log-derivative and of the Numerov results by factors ranging from 26 and 10, respectively, in the case of the high $v=12$ level to about 3.6 and 1.3 in the $v=3$ case. It follows from these factors that the errors in the hybrid log-derivative algorithms grow with energy much less rapidly than the errors in the two purely approximate solution algorithms. Analyzing more closely energy dependence of the errors listed in Table V one can find that in cases with $v=3$ to $v=6$ the nonhybrid log-derivative and the Numerov errors are approximately proportional to third power of respective $(\epsilon^D_v - V^{\min}_D)$ energies (with $V^{\min}_D = -0.65$ a.u., cf. Table I); the dependence of the hybrid log-derivative errors on these energies is close to linear. A theoretical justification of these findings is given in Appendix B.

TABLE V. Energies $\epsilon^D_v$ determined as poles of $T_{(Dv)}$ $(E,\lambda=0)$. Errors[a] of results obtained by the nonhybrid (nH) and half-hybrid (hH) log-derivative algorithms and by the Numerov (N) algorithm.

| | | | $\epsilon^D_v(\text{exact}) - \epsilon^D_v$ | | |
|---|---|---|---|---|---|
| $v$ | $\epsilon^D_v$ (exact) | $h$[b] | nH | hH | N |
| 3 | −0.616 812 379 | 0.04 | 101.9 | 28.1 | 37.8 |
| | | 0.02 | 6.2 | 1.7 | 2.2 |
| | | 0.01 | 0.3 | 0.0 | 0.1 |
| 4 | −0.608 555 072 | 0.04 | 181.3 | 32.9 | 76.2 |
| | | 0.02 | 11.2 | 2.0 | 4.2 |
| | | 0.01 | 0.7 | 0.1 | 0.3 |
| 5 | −0.600 842 311 | 0.04 | 280.1 | 36.3 | 103.8 |
| | | 0.02 | 17.2 | 2.2 | 6.4 |
| | | 0.01 | 1.1 | 0.1 | 0.3 |
| 6 | −0.593 673 994 | 0.04 | 391.3 | 38.5 | 144.8 |
| | | 0.02 | 24.0 | 2.3 | 8.9 |
| | | 0.01 | 1.4 | 0.1 | 0.5 |
| 8 | −0.580 970 692 | 0.04 | 615.5 | 39.9 | 227.2 |
| | | 0.02 | 37.8 | 2.4 | 14.1 |
| | | 0.01 | 2.3 | 0.1 | 0.9 |
| 12 | −0.562 097 424 | 0.04 | 824.7 | 31.2 | 303.0 |
| | | 0.02 | 50.3 | 1.9 | 18.7 |
| | | 0.01 | 3.0 | 0.0 | 1.1 |

[a] Given in $10^{-8}$ a.u.

[b] Step size (in a.u.). The integration range $[x_0, x_\infty]$ was [0.001,6.0] a.u. in the cases with $v=3$ to $v=6$ and $x_\infty = 10$ a.u. in the $v=8$, 12 cases.

To conclude the comparison of the algorithms, an estimation of their relative efficiency should be given. To facilitate this task, the list of matrix operations required at each step (or half-sector) is enclosed in Table VI. Restricting the count of operations to matrix inversions only one gets the factor of 4/3 for the ratio of the number of scalar operations per step required in the Numerov algorithm to the number of operations per half-sector in the nonhybrid log-derivative

TABLE VI. Summary of matrix operations[a] per step (or half-sector) in evaluation of an $N_0 \times N_0$ matrix of second-order transition amplitudes (or $J^0$-type integrals) involving an $N$-channel Green's function [Eq. (10)].

| | Log-derivative | | | |
|---|---|---|---|---|
| | nH | hH | H | Numerov |
| Inversions of symmetric $N \times N$ matrices | 3/2 | 3/2 | 3/2 | 2 |
| Multiplications of $N \times N$ by $N \times N_0$ matrices | 3/2 | 3/2 | 1 | 3 |
| Multiplications of $N \times N$ by diagonal matrices | 3/2 | 7/2 | 7/2 | 1 |

[a] Listed are only the matrix operations which scale like $N^3$ and $N^2$ in scalar operations.

algorithm. Obviously, this factor considerably underestimates the real requirements of the Numerov algorithm in cases involving small matrices (the effort connected with the other matrix operations listed in Table VI cannot be neglected in such cases). Still, it is larger than the factor $(2.67)^{1/4}$ being the ratio of the total number of half-sectors to the total number of steps required by the log-derivative and by the Numerov algorithms, respectively, to achieve the same accuracy in evaluation of a $T_{(iv)}$ integral. In effect, the nonhybrid log-derivative algorithm appears to be even slightly more efficient than the Numerov algorithm. Validity of this conclusion does not seem to be restricted to the present problem only. The same factor of 2.67 relating errors of $J^0$-type integrals generated by the two algorithms compared here was found, e.g., on the test problem of Ref. 22 (see Appendix A).

The half-hybrid algorithm requires the same number of matrix inversions in one half-sector as the nonhybrid version but two more multiplications of $N \times N$ matrices by diagonal matrices and, additionally, $N$ evaluations of trigonometric or hyperbolic functions. This does not seem to involve much more scalar operations than all the matrix operations to be performed at each step in the Numerov algorithm. Thus, relative efficiency of these algorithms is adequately measured by the ratio of numbers of steps required by them to achieve the same accuracy of results, i.e., by the factor

(error of "LD" result/error of "$N$" result)$^{1/4}$.

Applying this measure to the errors listed in Table V one can state that the half-hybrid log-derivative algorithm was about two times more efficient than the two other, nonhybrid log-derivative and Numerov algorithms in determination of the high energy level $\epsilon^D_{v=12}$ and all three algorithms were almost equally efficient in determination of the low energy level $\epsilon^D_{v=3}$.

## V. APPLICATION TO CALCULATION OF NONADIABATIC SHIFTS OF ROVIBRATIONAL ENERGY LEVELS IN THE $B\,^1\Sigma_u^+$, $B'\,^1\Sigma_u^+$, $C\,^1\Pi_u$, AND $D\,^1\Pi_u$ STATES OF $H_2$

The methods of finding nonadiabatic (corrections to) energies of bound rovibrational states, tested in the previous section on the model Hamiltonian, will be applied here to the Hamiltonian describing exactly the nuclear motion of $H_2$ on the manifold of the electronic states: $B$, $B'$, $C$, and $D$, affected by homogeneous ($\Sigma^+$–$\Sigma^+$, $\Pi$–$\Pi$) and heterogeneous ($\Sigma^+$–$\Pi^+$) nonadiabatic interactions. This Hamiltonian takes the form of the matrix operator,

$$\mathbf{H} = \begin{pmatrix} \mathbf{H}^{\Sigma\Sigma} & \mathbf{H}^{\Sigma\Pi} \\ \mathbf{H}^{\Pi\Sigma} & \mathbf{H}^{\Pi\Pi} \end{pmatrix},$$

with the following elements:

$$\mathbf{H}^{\Lambda\Lambda}_{i,j} = \delta_{i,j} H^i - 1/(2\mu)\left[2\mathbf{A}^{\Lambda}_{i,j}(R)\frac{d}{dR} + \mathbf{B}^{\Lambda}_{i,j}(R)\right] \times (1-\delta_{i,j}), \tag{58a}$$

where

$$H^i = -1/(2\mu)\left[\frac{d^2}{dR^2} - J(J+1)/R^2 + \mathbf{B}^{\Lambda}_{i,j}(R)\right] + V^i(R) \tag{58b}$$

for $i,j = B,B'$ if $\Lambda = \Sigma$, and $i,j = C,D$ if $\Lambda = \Pi$,

and

$$\mathbf{H}^{\Sigma\Pi}_{i,j} = 1/(2\mu)[2J(J+1)]^{1/2}\mathbf{L}_{i,j}(R) \tag{58c}$$

for $i = B,B'$, $j = C,D$ ($\Pi^+$ symmetry only).

Obviously, $H^i$ for $i = B,B',C,D$, are the corresponding Hamiltonians in the adiabatic approximation with $V^i$ denoting the Born–Oppenheimer potentials and with $-1(2\mu)\mathbf{B}^{\Lambda}_{i,j}$ standing for the adiabatic corrections to them. $\mathbf{A}^{\Lambda}_{i,j}$, $\mathbf{B}^{\Lambda}_{i,j}$, and $\mathbf{L}_{i,j}$ are matrix elements between the respective BO electronic functions of the nonadiabatic coupling operators.[19] The energy levels of the adiabatic Hamiltonians $H^i$ and the corresponding eigenfunctions will be denoted by $\epsilon^i_{vJ}$ and $\chi^i_{vJ}$, respectively, and the shifted energy levels, i.e., the eigenvalues of $\mathbf{H}$, will be denoted by $E^{i\Lambda^p}_{vJ}$ with $p(=+,-)$ being the parity index. Since the coupling $\mathbf{H}^{\Sigma\Pi}$ is inactive between the $\Sigma^+$ and the $\Pi^-$ states the $E^{i\Pi^-}_{vJ}$ energies, for $i = C,D$, are eigenvalues of the $\mathbf{H}^{\Pi\Pi}$ block only.

The nonadiabatic shifts, $E^{i\Lambda^p}_{vJ} - \epsilon^i_{vJ}$, were calculated with the new methods for a number of $(v,J)$ levels in the $i = B,B'$ states and in the $i = C,D$ states of $\Pi^+$ and $\Pi^-$ symmetry using on input the *ab initio* results of Ref. 19 for the BO potentials, the adiabatic corrections, and for the nona-

TABLE VII. Nonadiabatic shifts (in $cm^{-1}$) of selected rovibrational energy levels in the $B$, $B'$, $C$, and $D$ states of $H_2$. Comparison with results of Ref. 13 obtained by the renormalized Numerov method.

| | | $E^{i\Sigma^+}_{v,J=0} - \epsilon^i_{v,J=0}$ | | | | | $E^{i\Pi^-}_{vJ} - \epsilon^i_{vJ}$ | |
|---|---|---|---|---|---|---|---|---|
| $i$ | $v$ | | Ref. 13 | $i$ | $J$ | $v$ | | Ref. 13 |
| $B$ | 0 | −0.14 | −0.13 | $C$ | 1 | 0 | −0.03 | −0.03 |
| | 10 | −1.26 | −1.26 | | | 2 | −0.13 | −0.13 |
| | 20 | −1.38 | −1.37 | | | 6 | −0.19 | −0.19 |
| | 28 | −1.16 | −1.15 | | | 7 | −0.195 | −0.19 |
| $B'$ | 0 | 0.29 | 0.29 | | | 9 | −0.185 | −0.18 |
| | 2 | 0.91 | 0.91 | | 4 | 6 | −0.19 | −0.19 |
| | 4 | 0.98 | 0.99 | $D$ | 1 | 0 | 0.04 | 0.04 |
| | 5 | 0.65 | 0.66 | | | 1 | 0.09 | 0.10 |
| | 6 | 0.075 | 0.08 | | | 2 | 0.13 | 0.13 |
| | 7 | 0.10 | 0.10 | | 5 | 1 | 0.09 | 0.09 |

TABLE VIII. Results of calculations of nonadiabatic shifts[a] $E_{vJ}^{D\Pi^+} - \epsilon_{vJ}^{D}$ in the $D$ state of $H_2$ for $(vJ)$ levels in energy range below dissociation limit of the $B$, $B'$, and $C$ states.

| | | Pertubative[b] | | | Nonperturbative | | |
|---|---|---|---|---|---|---|---|
| $J$ | $v$ | $(B,B')+D$[c] | | | $(B,B',D)$ | $(B,B',C,D)$ | Ref. 13 $(B,B',C,D)$ |
| 1 | 0 | 3.84 | 3.82 | (2) | 3.81 | 3.85 | 3.85 |
| | 1 | 1.68 | 1.67 | (2) | 1.67 | 1.77 | 1.78 |
| | 2 | 4.10 | 4.05 | (2) | 4.05 | 4.18 | 4.17 |
| 2 | 0 | 11.11 | 10.96 | (2) | 10.92 | 10.95 | 10.95 |
| | 1 | 4.60 | 4.54 | (3) | 4.53 | 4.63 | 4.66 |
| | 2 | 10.95 | 10.64 | (3) | 10.62 | 10.74 | 10.75 |
| 3 | 0 | 21.10 | 20.59 | (3) | 20.48 | 20.50 | 20.50 |
| | 1 | 7.84 | 7.61 | (3) | 7.55 | 7.65 | 7.72 |
| | 2 | 18.45 | 17.64 | (3) | 17.71 | 17.73 | 17.75 |
| 4 | 0 | 32.90 | 31.75 | (3) | 31.51 | 31.54 | 31.54 |
| | 1 | 9.65 | 9.10 | (4) | 8.83 | 8.97 | 9.08 |
| | 2 | 24.00 | 22.43 | (4) | 22.44 | 22.58 | 22.63 |
| 5 | 0 | 45.20 | 43.48 | (3) | 43.09 | 43.13 | 43.13 |
| | 1 | 6.50 | 5.78 | (4) | 4.70 | 4.91 | 5.10 |
| | 2 | 21.85 | 19.26 | (4) | 19.15 | 19.34 | 19.47 |

[a] The shifts are given in $cm^{-1}$.

[b] Results by formulas (60)–(60b); for each $vJ$ level are listed: the second-order perturbation result (obtained for $k=1$) and the result converged with respect to iterations over energy; the number of iterations is given in parentheses.

[c] The states included in calculations.

diabatic couplings. Cubic splines were employed to interpolate between the *ab initio* points. The respective $T$ integrals [cf. Eq. (54)]

$$T_{(ivJ)}(E) = \langle \varphi_{vJ}^{i}, 1/E - \mathbf{H})\varphi_{vJ}^{i}\rangle \quad \text{with} \quad (\varphi_{vJ}^{i})_j = \delta_{i,j}\chi_{vJ}^{i}, \tag{59}$$

and $E_{\text{shift}}^{(DvJ)}$ integrals [cf. Eq. (52)], in the perturbative treatment of the $D$ state levels;

$$(E_{\text{shift}}^{(DvJ)})^{(k)} = \langle \varphi_{vJ}^{D}, 1/(E^{(k-1)} - \mathbf{H}^{\Sigma\Sigma})\varphi_{vJ}^{D}\rangle, \tag{60}$$

where

$$(\varphi_{vJ}^{D})_j = \mathbf{H}_{j,D}^{\Sigma\Pi}\chi_{vJ}^{D}, \quad j = B,B', \tag{60a}$$

$$E^{(k)} = E^{(k-1)} + (E_{\text{shift}})^{(k)}, \quad E^{(0)} = \epsilon_{vJ}^{D}, \tag{60b}$$

were evaluated using the step size $h = 0.005$ a.u.; the maximal integration range was [0.001, 20.0] a.u. The results obtained for the energy shifts are compared in Tables VII and VIII with the results of the recent calculations by Senn, Quadrelli, and Dressler[13] in which the same Hamiltonian was dealt with, except perhaps for small differences in the shape of the $V^i(R)$ and of the $\mathbf{A}_{ij}^{\Lambda}(R)$ functions (as they might follow from the use of the different procedure for interpolation of the *ab initio* data), and the eigenvalues were determined by the well-established renormalized Numerov technique.[3] The comparison shows quite good agreement of the results for the shifts caused by the homogeneous interactions only; $E_{vJ}^{i\Pi^-} - \epsilon_{vJ}^{i}$ for $i = C,D$, and $E_{vJ=0}^{i\Sigma^+} - \epsilon_{vJ=0}^{i}$ for $i = B,B'$. The discrepancies do not exceed the value of $-0.01$ $cm^{-1}$. Larger discrepancies are seen between the present nonperturbative four-state results and the results of Ref. 13 for the $E_{vJ}^{D\Pi^+} - \epsilon_{vJ}^{D}$ shifts (Table VIII), especially in the $J=5$ $v=1$ and $v=2$ cases ($-0.19$ and $-0.13$ $cm^{-1}$, respectively). These discrepancies are believed to be caused by some differences in the couplings used rather than by any deficiencies of our procedure of localization of the eigenvalues of $\mathbf{H}$.

The perturbative treatment applied here to the $D$-state levels below the dissociation limit of the $B$, $B'$, and $C$ states—analogous to the treatment applied previously[12] to levels above this threshold—is shown in Table VIII to give quite accurate results in all cases [the errors relative to the nonperturbative $(B,B',C)$ results are of order of 1%] except for the $v=1$ $J=5$ and $J=4$ cases (the errors are 20% and 3%, respectively). It is shown also that the iteration over energy, as indicated in the formulas (60)–(60b) improves considerably the second-order perturbation theory results obtained at the first step.

TABLE IX. Resonances in Woods–Saxon potential.[a] Absolute errors[b] $E_{\text{ref}} - E_{\text{calc}}$ of the results by the log-derivative and by the Numerov algorithms.

| | | Log-derivative | | Numerov[c] | | | |
|---|---|---|---|---|---|---|---|
| $E_{\text{ref}}$ | $h$ | nonhybrid | hybrid | $S_0$ | $S_1$ | $S_2$ | $S_3$ |
| 53.588 872 | 1/16 | | 206 | −230 727 | 5 350 | −1205 | 58 |
| | 1/32 | 37 860 | 12 | −14 110 | 342 | −75 | 3 |
| | 1/64 | 2 342 | 0 | −879 | 21 | −4.5 | 0 |
| 341.495 874 | 1/16 | | 2032 | | 566 566 | −35 267 | 28 |
| | 1/32 | | 65 | −7 536 068 | 34 380 | −1 979 | 14 |
| | 1/64 | 1 185 614 | 4 | −436 825 | 2 147 | −121 | 1 |
| | 1/128 | 72 937 | | −27 127 | 135 | −7 | |
| 989.701 916 | 1/16 | | 3580 | | | −394 003 | −5147 |
| | 1/32 | | 253 | | 717 405 | −16 064 | 17 |
| | 1/64 | | 11 | | 43 730 | −927 | 3 |
| | 1/128 | 4 417 705 | | −1 637 376 | 2 739 | −53 | |

[a] Test problem of Ref. 20: $[d^2/dx^2 + E - V(x)]\psi(x) = 0$, $V(x) = u_0/(1+t) + u_1 t/(1+t)$, $t = \exp[(x-x_0)/a_0]$, $u_0 = -50$; $a_0 = 0.6$; $x_0 = 7$; $u_1 = -u_0/a_0$; $[x',x''] = [0,15]$.

[b] Given in $10^{-8}$ units.

[c] Results of Refs. 20 and 21. $S_k$ with $k = 1, 2, 3$ are the versions of the Numerov algorithm discussed in these papers. $S_0$ corresponds to the original scheme.

## ACKNOWLEDGMENTS

The author thanks Professor K. Dressler for sending her a preprint of Ref. 13 and Dr. D. E. Monolopoulos for a copy of his Ph.D. thesis. This work was supported in part by the Polish Ministry of National Education Project CPBP 01.06.

## APPENDIX A: AN INVARIANT IMBEDDING NUMEROV-RELATED ALGORITHM FOR EVALUATION OF THE $J^{\alpha}_{x',x''}$ INTEGRALS [CF. EQ. (3)]

In order to derive such an algorithm, the text-book formulations of the invariant imbedding theory, e.g., that of Ref. 5, can be directly exploited.

The derivation starts with considering the following boundary value problems for three-point difference equations resulting from applying the Numerov or a Numerov-like (cf. Ref. 20) discretization scheme to the differential equations for the functions $\psi^{\alpha}_{x',x''}(x)$, with $\alpha = -,0$, i.e., to Eqs. (2) and (2a):

$$U^{\alpha}(k,M) - Q_k U^{\alpha}(k,M) + U^{\alpha}(k-1,M) = \delta_{\alpha,0}(G_{k+1} + b_1/b_0 G_k + G_{k-1}), \tag{A1}$$

$$U^{-}(0,M) = 0, \quad U^{-}(M,M) = I,$$
$$U^{0}(0,M) = U^{0}(M,M) = 0, \tag{A2}$$

where

$$U^{\alpha}(k,M) := [I + b_0 B(x_k)]\psi^{\alpha}_{x',x''}(x_k) \times [I - \delta_{\alpha,-} b_0 B(x_M)]^{-1}, \tag{A3}$$

$$Q_k := -[a_1 + b_1 B(x_k)][I + b_0 B(x_k)]^{-1}, \tag{A4}$$

$$G_k := b_0 \phi(x_k), \tag{A5}$$

$$x_k = x_0 + kh, \quad x_0 := x', \quad x_M := x''. \tag{A6}$$

In the original Numerov scheme, employed here, the coefficients $a_1$, $b_0$, and $b_1$ assume the values

$$a_1 = -2, \quad b_0 = h^2/12, \quad b_1 = 5/6\, h^2. \tag{A7}$$

Next, the sequence of analogous problems for $U^{\alpha}(k,l)$ with $0 \leqslant l \leqslant M$ is introduced and the superposition relations connecting solutions of these problems:

$$U^{\alpha}(k,l) = U^{-}(k,l-1)U^{\alpha}(l-1,l) + \delta_{\alpha,0} U^{0}(k,l-1) \quad \text{for } \alpha = -,0 \tag{A8}$$

are exploited to establish the corresponding recurrence relations for the following quantities:

$$R_l := U^{-}(l,l+1), \tag{A9}$$

$$S_l := U^{0}(l,l+1), \tag{A10}$$

$$I^{\alpha}_l := \sum_{k=0}^{l} \omega_k \{[I + b_0 B(x_k)]^{-1} U^{\alpha}(k,l)\}^T \phi(x_k) \quad \text{for } \alpha = -,0, \tag{A11}$$

where $\omega_k = h$ for $k \neq 0,M$ and $\omega_0 = \omega_M = h/2$. These relations are the basic constituents of the algorithm for the required integrals:

$$R_0 = 0, \quad I^{-}_0 = 0, \quad I^{0}_0 = 0, \quad S_{-1} = 0, \tag{A12}$$

$$S_{l-1} = R_{l-1}[S_{l-2} - b_0(\phi_l + b_1/b_0 \phi_{l-1} + \phi_{l-2})] \quad [\phi_l := \phi(x_l)], \tag{A13}$$

$$I^{0}_l = (S_{l-1})^T I^{-}_{l-1} + I^{0}_{l-1}, \tag{A14}$$

$$q_l = [c + c b_0 B_l] \quad [B_l := B(x_l)], \tag{A15}$$

$$I^{-}_l = R_{l-1} I^{-}_{l-1} + W_l q_l \phi_l, \tag{A16}$$

$$R_l = (q_l - R_{l-1} - 10)^{-1} \quad \text{for } l = 1,2,3\ldots,M, \tag{A17}$$

$$J^{-}_{x',x''} = (c q_M)^{-1} I^{-}_M, \tag{A18}$$

$$J^{0}_{x',x''} = I^{0}_M, \tag{A19}$$

where

$$c := b_0/(b_1 - a_1 b_0), \quad W_l := c\omega_l. \tag{A20}$$

This algorithm bears strong similarity to the algorithm presented in Ref. 22. (Indeed, applied to the test problem of that paper, it gave results of the same accuracy, although only one-way integrations were carried out.) However, definitely less matrix operations are required. Therefore testing the new log-derivative algorithms vs the above Numerov-related algorithm was believed to give a more stringent proof of their quality.

It would be highly interesting to learn how the log-derivative algorithms would compare with algorithms based on the Numerov-like schemes adapted to Schrödinger equation, as described in Ref. 20. Some information concerning this question is provided in Table IX where both the hybrid and the original log-derivative algorithms, the original Numerov, and the three Numerov-like schemes of Ref. 20 are compared with respect to accuracy yielded in one channel calculations of several resonances in the Woods–Saxon potential. It is demonstrated that of all the Numerov-related algorithms only the $S_3$ scheme, maximally adapted to the Schrödinger equation, compares favorably with the hybrid log-derivative algorithm. Obviously, more accuracy tests, also tests on many channel problems, and an estimation of the number of operations needed at a single step (including the operations connected with evaluation of the $b_0$, $b_1$, and $a_1$ coefficients of Ref. 20) are necessary in order to state whether the algorithm (A12)–(A20) based on the $S_3$-Numerov scheme would be more efficient than the hybrid log-derivative algorithm in application to problems of physical interest.

## APPENDIX B: ENERGY DEPENDENCE OF DISCRETIZATION ERRORS IN THE HYBRID AND IN THE NONHYBRID LOG-DERIVATIVE ALGORITHMS

Expressions will be derived for errors of the half-sector $L$ matrices arising from the discretization of the sector integral equations [cf. Eqs. (16) and (16a)]:

$$\psi^{\alpha}_{[p]}(x) = \varphi^{\alpha}_{[p]}(x) - \int_{x_{2p-2}}^{x_{2p}} G^{0}_{[p]}(x,y) B^{p}(y) \psi^{\alpha}_{[p]}(y)\, dy \quad \text{for } \alpha = +,-, \tag{B1}$$

where

$$G^{0}_{[p]}(x,y) = W^{-1} \varphi^{-}_{[p]}(x_<) \varphi^{+}_{[p]}(x_>) \tag{B2}$$

by means of the modified Simpson formula:

$$\int_{\bar{y}-h}^{\bar{y}+h} f(y)dy = h/3[f(\bar{y}-h) + 4f(\bar{y}) + f(\bar{y}+h)] + h^2/6[f_+^{(1)}(\bar{y}) - f_-^{(1)}(\bar{y})] + R. \tag{B3}$$

$R$ is the error of this formula

$$R = -h^4/72[f_+^{(3)}(\bar{y}) - f_+^{(3)}(\bar{y})] - h^5/90 f^{(4)}(\xi), \tag{B4}$$

where $\xi$ denotes a point from the interval $[\bar{y}-h, \bar{y}+h]$ and

$$f_\pm^{(k)}(\bar{y}) := \lim_{\epsilon \to 0^+} \frac{d^k}{dy^k} f(y)|_{y=\bar{y}\pm\epsilon}. \tag{B5}$$

The form of the leading term, i.e., of the $h^4$ term, in this discretization error (cf. Ref. 11 for its derivation) is crucial for analyzing energy dependence of the corresponding errors of the half-sector $L$ matrices. Before proceeding to this analysis, however, let us point out an important difference in the form of the integral equations (B1) and (B2) to be discretized, using also the $h^4$ term, in order to obtain expressions appropriate for the hybrid and for the nonhybrid $L$ matrices. The difference stems, of course, from the use of the reference potentials $B^p_{\rm ref}$ in the hybrid case. They encompass the entire energy dependence of the coupling matrix $B$ because energy occurs usually as an additive constant in this matrix. Thus, the "rest" coupling $B^p$ occuring in Eq. (B1) is energy independent in the hybrid case; the energy constant is entirely included into the functions $\varphi^{\pm}_{[p]}$ [cf. Eqs. (16) and (16a)] from which the (diagonal) matrix $G^0_{[p]}$ is built.

Introducing an abbreviated notation for the integrand in the integral equations (B1) at $x = x_{2p-1} := \bar{x}$ and suppressing, for the sake of clarity, all the indices;

$$G(\bar{x},y)U(y)\psi(y) := G(\bar{x},y)t(y) := f(y), \qquad U := B - B_{\rm ref}, \tag{B6}$$

one can simply write down the expressions necessary for inclusion of the $h^4$ term when applying the quadrature formula (B3) to these equations:

$$f_+^{(3)}(\bar{x}) - f_-^{(3)}(\bar{x}) = \bar{G}^{(3)}(\bar{x})t(\bar{x}) + 3\bar{G}^{(1)}(\bar{x})t^{(2)}(\bar{x}). \tag{B7}$$

$\bar{G}^{(k)}(\bar{x})$ denotes the discontinuity of $d^k/dy^k G(\bar{x},y)$ at $y=\bar{x}$, i.e.,

$$\bar{G}^{(k)}(\bar{x}) := G_+^{(k)}(\bar{x},\bar{x}) - G_-^{(k)}(\bar{x},\bar{x}). \tag{B8}$$

Obviously, no discontinuities occur in the zeroth and in the second derivatives which has been already exploited in the above expression. The discontinuities in the first and in the third derivatives are

$$\bar{G}^{(1)}(\bar{x}) = I, \quad \bar{G}^{(3)}(\bar{x}) = -B_{\rm ref} \quad [B_{\rm ref} := \operatorname{diag} B(\bar{x})]. \tag{B9}$$

Taking into acount the last two equalities and saving from $t^{(2)}$ only the most strongly energy-dependent part, $U\psi^{(2)}$:

$$U\psi^{(2)} = -UB\psi = -U(B_{\rm ref} + U)\psi, \tag{B10}$$

one obtains

$$f_+^{(3)}(\bar{x}) - f_-^{(3)}(\bar{x}) \approx -W(\bar{x})\psi(\bar{x}) \approx \hat{W}(\bar{x})\psi(\bar{x}), \tag{B11}$$

where

$$W(\bar{x}) := B_{\rm ref}U(\bar{x}) + 3U(\bar{x})[B_{\rm ref} + U(\bar{x})], \tag{B12}$$

$$\hat{W} := 1/2(W + W^T). \tag{B13}$$

The second approximation, the symmetrization of the matrix $W$, not influencing essentially the energy dependence of the $(f_+^{(3)} - f_-^{(3)})$ term, is introduced for convenience only. Eventually, the discretization of the integral equations (B1) by means of the formula (B3) with the $h^4$ term (approximately) included leads to the algebraic equations:

$$\hat{F}^{\alpha}_{[p]}(x_i) = \hat{\varphi}^{\alpha}_{[p]}(x_i) - \sum_{k=2p-2}^{2p} \omega_k G^0_{[p]}(x_i,x_k) \times \hat{q}^p_k B^p(x_k)\hat{F}^{\alpha}_{[p]}(x_k), \tag{B14}$$

$$\hat{F}^{\alpha}_{[p]}(x_i) := (\hat{q}^p_i)^{-1}\psi^{\alpha}_{[p]}(x_i) \quad \text{for} \quad \alpha = +,- \text{ and } i = 2p-2, 2p-1, 2p, \tag{B15}$$

which differ from the equations considered in the derivation of the log-derivative algorithms [cf. Eqs. (19) and (19a)] only because an extra term appears in the formula defining the matrix $\hat{q}^p_k$ as compared with the formula for the matrix $q^p_k$ [cf. Eq. (19b)]:

$$\hat{q}^p_k := [I + (q^p_k)^{-1} + \eta_k \hat{W}^p_k]^{-1}, \tag{B16}$$

where

$$\hat{W}^p_k := 2[B^p(x_k)B^p_{\rm ref} + B^p_{\rm ref}B^p(x_k)] + 3[B^p(x_k)]^2, \tag{B17}$$

$$\eta_k = h^4/72 \ (0) \quad \text{for } k \text{ odd (even)}. \tag{B18}$$

Thus, further steps of the procedure presented in Ref. 8 can be applied to these equations without any modification giving the required expressions for the half-sector $L$ matrices, $\hat{L}_{l,l+1}$, for $l = 2p-2, 2p-1$, which again differ from the expressions for the corresponding matrices $L_{l,l+1}$, i.e., from Eqs. (22a)–(22d), only in that the matrix $q^p_l$ is replaced by the matrix $\hat{q}^p_l$. Having established this fact one can finally estimate the errors of the matrices $L_{l,l+1}$; $\hat{L}_{l,l+1} - L_{l,l+1}$, which are fully determined by the following differences [cf. Eq. (22a)]:

$$\hat{S}^p_k - S^p_k = \tilde{\omega}_k(\hat{q}^p_k - q^p_k)B^p_k \quad \text{for } k = l, l+1. \tag{B19}$$

The result is

$$\hat{S}^p_k - S^p_k \approx \tilde{\omega}_k \eta_k \hat{W}^p_k B^p_k. \tag{B20}$$

It remains to point out that these differences depend linearly on the reference potentials $B^p_{\rm ref}$ which, when used, carry the energy constant. When the reference potentials are not used the energy constant remains in the matrices $B^p(x_k)$ (since $B^p = B$ in this case) and these matrices appear in third power in the above formula [cf. Eq. (B17)].

Since the half-sector $L$ matrices are the basic quantities of all the log-derivative algorithms and are accumulated in the same way in the hybrid and in the nonhybrid versions the above analysis is considered sufficient to explain the findings of the tests described in Sec. IV.

[1]S. J. Singer, S. Lee, K. F. Freed, and Y. B. Band, J. Chem. Phys. **87**, 4762 (1987).
[2]J. C. Light, and R. B. Walker, J. Chem. Phys. **65**, 4272 (1976).
[3]B. R. Johnson, J. Chem. Phys. **67**, 4086 (1978); **69**, 4678 (1978).
[4]J. Casti and R. Kalaba, *Imbedding Methods in Applied Mathematics* (Addison-Wesley, Reading, MA, 1973).
[5]E. Angel and R. Bellman, *Dynamic Programming and Partial Differential Equations* (Academic, New York, 1972).
[6]F. Mrugala, J. Comput. Phys. **58**, 113 (1985).
[7]B. R. Johnson, J. Comput. Phys. **13**, 445 (1973).
[8]F. Mrugala and D. Secrest, J. Chem. Phys. **78**, 5954 (1983).
[9]F. Mrugala and D. Secrest, J. Chem. Phys. **79**, 5960 (1983).
[10]D. E. Manolopoulos, J. Chem. Phys. **85**, 6425 (1986).
[11]D. E. Manolopoulos, Ph.D. thesis, University of Cambridge, 1988.
[12]F. Mrugala, Mol. Phys. **65**, 377 (1988).
[13]P. Senn, P. Quadrelli, and K. Dressler, J. Chem. Phys. **89**, 7401 (1988).
[14]D. M. Sloan and J. S. Bramley, J. Comput. Phys. **30**, 296 (1979).
[15]R. E. Bellman and R. E. Kalaba, Proc. Natl. Acad. Sci. **42**, 629 (1956).
[16]D. Secrest and B. R. Johnson, J. Chem. Phys. **45**, 4556 (1966).
[17]U. Fano, Phys. Rev. **124**, 1866 (1961).
[18]F. T. Smith, Phys. Rev. **118**, 349 (1960).
[19]L. Wolniewicz and K. Dressler, J. Chem. Phys. **88**, 3861 (1988).
[20]L. Gr. Ixaru and M. Rizea, J. Comput. Phys. **73**, 306 (1987).
[21]L. Gr. Ixaru, Comput. Phys. Commun. **20**, 97 (1980).
[22]L. Wolniewicz, J. Comput. Phys. **40**, 440 (1981).